POLITECNICO DI MILANO

FACULTY OF INDUSTRIAL AND INFORMATION ENGINEERING

MASTER DEGREE COURSE IN ENERGY ENGINEERING

Research on Grid-connected and Islanding Control Strategy of AC/DC Hybrid Microgrid in a Small Plant

Master's Thesis

Supervisor: Prof. Enrico Tironi

Author:

Zhenghong Chen Matr. 854627

Academic Year 2017-2018

INDEX

INDEX OF FIGURES

INDEX OF TABLES

ABSTRACT

Abstract in italiano

Con l’esaurirsi dei combustibili fossili e il deterioramento delle condizioni ambientali, sempre maggiore attenzione ricade sulla questione dell’approvvigionamento energetico e sulla sua primaria importanza. Le microreti in particolare hanno conosciuto un importante sviluppo in quanto sono considerate un sistema in grado di raggruppare efficacemente nuove fonti energetiche, dispositivi di accumulo e carichi. Le microreti ibride CA/CC contengono sia sbarre in CA che in CC. Rispetto alle tradizionali microreti in CA e alle più recenti microreti in CC, le microreti ibride riescono efficacemente a ridurre il numero di stadi di conversione in cascata, migliorare la qualità della fornitura e l’utilizzazione dell’energia. Inoltre, la gestione delle microreti ibride può essere significativamente più flessibile. Per queste ragioni, le microreti ibride sono considerate il futuro delle microreti.

Questa tesi è focalizzata sulle strategie di controllo delle microreti ibride CA/CC. Vengono discusse diverse strategie di controllo in diversi modi operativi delle microreti ibride e, in particolare, si propone una nuova strategia di controllo basata su statismi generalizzati per l’intera rete che consente la gestione in isola delle porzioni in CA e CC. In accordo con quanto previsto dalla strategia di controllo proposta, viene inoltre presentata la ricerca svolta sulle transizioni morbide (cosiddette “smooth transition”) tra differenti modi operativi.

In primo luogo, la struttura di una microrete ibrida CA/CC che comprende un impianto fotovoltaico, batterie, celle a combustibile e carichi a potenza costante viene introdotta considerando un piccolo impianto; un modello di simulazione viene definito tramite PSCAD/EMTDC.

In seconda battuta, vengono analizzate le strategie di controllo delle microreti ibride CA/CC nei diversi modi operativi. Per risolvere i problemi delle strategie di controllo tradizionali, quali distribuzione squilibrata del carico, forte dipendenza dalla struttura della microrete, dimensionamento eccessivo del convertitore di interconnessione ecc., si propone una nuova strategia di controllo basata su statismi generalizzati per l’intera rete (indifferentemente in CA o CC). Quando la microrete opera connessa alla rete di distribuzione, si sfrutta quest'ultima per mantenere un funzionamento stabile del sistema e sfruttare al massimo le fonti rinnovabili. Quando operata in isola, tutta la generazione distribuita controllabile fornisce supporto al sistema. La strategia di controllo proposta migliora la distribuzione del carico e rende il sistema più affidabile e espandibile; inoltre, realizza la cosiddetta connessione "plug-and-play" per la generazione distribuita. I risultati delle simulazioni svolte in ambiente PSCAD/EMTDC mostrano che, applicando la strategia di controllo proposta, la microrete ibrida CA/CC riesce a operare in modo stabile ed efficiente.

Infine, i metodi per ottenere una transizione morbida tra i diversi modi operativi sono studiati. Viene analizzata la struttura dei regolatori PI e viene discussa la causa dell'impatto delle transizioni tra modi operativi sul controllo della rete. Viene proposto un metodo per ottenere transizioni morbide basato su un segnale di passaggio all'operazione in isola. Rispetto ai metodi tradizionali per ottenere transizioni morbide, i risultati di simulazione provano che il metodo proposto permette di semplificare significativamente la taratura dei guadagni dei regolatori PI e di ottenere prestazioni migliori. Durante la transizione tra due modi operativi, la durata del transitorio è minore e l'effetto sulle grandezze elettriche è più contenuto. L'effetto del carico sulla transizione morbida tra modi operativi è studiato considerando il metodo proposto.

Parole chiave: Microgrid ibrido, Strategia di controllo, Controllo dello statismo, Commutazione fluida

Abstract in English

With the depletion of fossil energy and the deterioration of environmental, the issue of energy has received increasing attention as the primary issue. As an effective way to combine distributed generators(DGs), energy storage system(ESS) and loads, microgrid has developed a lot. The AC/DC hybrid microgrid contains both AC and DC buses. Compared with the traditional AC microgrid and novel DC microgrid, it can effectively avoid repeated power conversion, improve power quality and energy utilization. What's more, the operation can be more flexible. Hybrid microgrid has become the future of microgrid.

This thesis focuses on the control strategy of AC/DC hybrid microgrid. It discusses about different control strategies in different operation modes of hybrid microgrid, especially, the novel entire network droop control strategy for AC-DC mixed islanding mode is proposed. According to the proposed control strategy, research on smooth transition is also conducted.

Firstly, an AC/DC hybrid microgrid structure including PV cell, battery, fuel cell and constant power load is proposed in a small plant and an electromagnetic transient simulation model is established based on PSCAD/EMTDC.

Secondly, the control strategies of AC/DC hybrid microgrids in different operating modes are analyzed. To solve the problems of traditional control strategy such as unreasonable load distribution, heavy dependence on microgrid structure, excessive transmission power of interlink converter(ILC), etc., a novel entire network droop control strategy is proposed. In grid-connected mode, the microgrid is supported by utility grid to maintain stable operation of the system and make maximum use of renewable energy. In islanding mode, all controllable DGs provide support for the system. The proposed control strategy improves load sharing and makes the system more reliable and expandable. The "plug and play" of DGs is realized. The simulation results based on PSCAD/EMTDC show that by applying this control strategy, the AC/DC hybrid microgrid can operate stably and efficiently.

Finally, the smooth transition method between different operating modes is studied. The structure of PI regulator is analyzed and the reason of transition impact is discussed. A smooth transition method based on islanding signal is proposed. Compared with the traditional smooth transition method, the simulation results show that the proposed smooth transition method can greatly simplify the setting of the PI regulator’s parameters and achieve better smooth transition effects. During mode transition, the transient time is shorter and the electrical impact is smaller. The influence of load on smooth transition is also studied based on the novel smooth transition method.

Key words: Hybrid microgrid, Control strategy, Droop control, Smooth transition

1 INTRODUCTION

1.1 Background and significance

With the rapid development of society and economy, the demand for traditional fossil fuel has increased a lot. It brings a series of ecological and environmental problems, which runs counter to the concept of sustainable development. At the same time, limited fossil energy reserves have also become an urgent problem for future economic development. In order to solve these problems, people focus their attention on the development and utilization of new energy. However, the intermittent and distributed feature of new energy limit its development as a large-scale centralized power plant. What's more, centralized power stations are usually far away from load centre. Large-scale long-distance power transmission will not only reduce the power utilization rate, but also cause safety risks in power system. As a result, microgrid as a union of distributed power sources, energy storage systems, energy conversion devices, loads, monitoring and protection devices has attracted more and more attention.[1][2][3] Microgrid can exchange energy and information with utility grid in grid-connected mode. In addition, when fault occurs in utility grid, microgrid can work in islanding mode to ensure power supply of local loads, improving the reliability of power supply.[4][5]

Till now, a lot of research has been conducted on the operation, control and protection of traditional AC microgrids. In recent years, with the increase of DC power equipment such as mobile phones, computers, electric vehicles, frequency conversion devices and so on, the concept of DC microgrid has been proposed to reduce redundant AC-DC converters.[6][7] However, no matter traditional AC microgrids or novel DC microgrids cannot minimize unnecessary power transfer. As a result, the researchers proposed the concept of AC/DC hybrid microgrid.

The hybrid microgrid has both AC bus and DC bus. AC generators and AC loads are connected to AC bus while DC generators and DC loads are connected to DC bus.[8] In this way, the number of redundant converters can be reduced and power quality can be improved. AC bus and DC bus are connected through an interlink converter(ILC). Hybrid microgrid is suitable for all kinds of DGs and loads. The typical structure is shown in Figure 1-1.

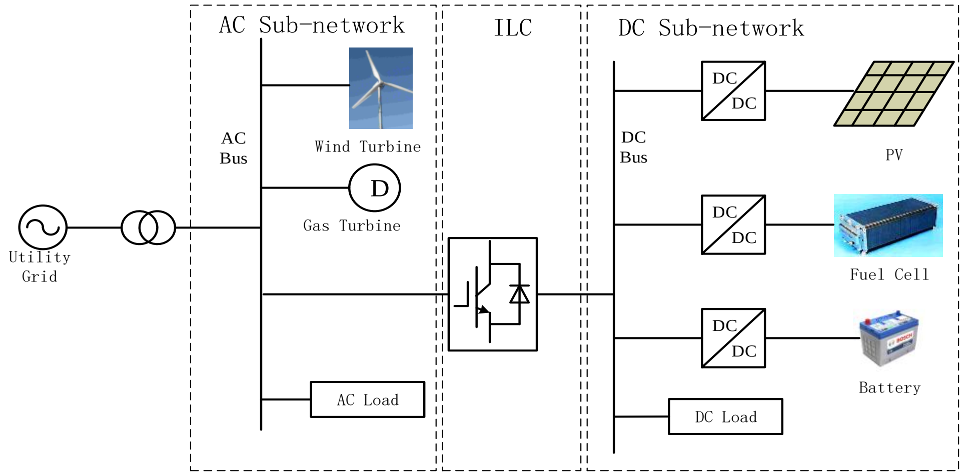

Figure 1- 1 Typical structure of hybrid microgrid.

DGs such as photovoltaic cell, wind turbine has been applied in microgrid in order to make full use of renewable energy. Because the output power is affected by the environment, microgrid needs to be equipped with energy storage devices (such as batteries, super capacitors, etc.) to suppress power fluctuations. However, energy storage devices are generally unable to charge and discharge for a long time. In order to improve the reliability of microgrid, controllable distributed power supply (such as fuel cells, micro-combustion engines, etc.) needs to be equipped in microgrid. AC/DC hybrid microgrid has advantages over AC or DC microgrid:

1) It avoids repeated conversion of electrical energy and improves power quality.

2) It reduces the use of various types of converters to save the cost of equipment.

3) The operation of AC/DC hybrid microgrid is more flexible. AC and DC sub-network can support each other in mixed islanding mode, which improves reliability of the system.

At present, the research of AC/DC hybrid microgrid is still at initial stage. The structure of hybrid microgrid, control strategy, energy management, etc. are the main problems in the application of AC/DC hybrid microgrids. The control strategy of the hybrid microgrid is of great significance. For this reason, this thesis focuses on the control strategy of hybrid microgrid.

1.2 Research status of microgrid

1.2.1 Overview of microgrid development

In 2001, RH Lasseter of the University of Wisconsin formally proposed the concept of microgrids. Subsequently, the Electric Reliability Solutions Association (CERTS) published document that clearly defined the concept of microgrids based on power electronics technology. The microgrid model consists of PV panel, wind turbine, small rotating equipment, various energy storage devices, etc. All DGs are connected to microgrid through power electronic devices. The key equipment is an intelligent static switchgear that controls the connection and disconnection of microgrid and utility grid. In 2003, the goal of "Power Grid Modernization" was put forward by President Bush. It aimed to realize intelligent the power grid through the application of information technology and communication technology. In "Grid 2030" development strategy, the U.S. Department of Energy formulated the development plan for the U.S. power system. Microgrid research is one of the important components of this strategy.

Due to the shortage of domestic resources, Japan has also conducted research on microgrids, but the research mainly focused on diversifying energy supplies, reducing pollution, and satisfying individualized power requirements of users. Japan has also subsumed the independent power system powered by conventional power supplies into the research of microgrids, which has greatly expanded the definition of microgrids proposed by CERTS. Based on this framework, Japan has established a number of microgrid projects. In addition, Japanese scholars have also proposed the Flexible Reliability and Intelligent Electrical Energy Delivery System (FRIENDS). The main idea is to add flexible AC transmission systems (FACTS) to distribution network to achieve the optimization of the distribution network's energy structure to meet users' multiple requirements. At present, Japan has taken this system as one of its important forms of microgrid.

In order to meet the requirements of the electricity market, guarantee safe power supply and protect the environment, the EU put forward a "smart grid" development plan in 2005. In 2006, specific technical implementation guidelines were made for the plan. As an European power development target for 2020, the plan points out that future European power grids requires to be flexible, accessible, reliable, and economical. During 2006-2010, the EU launched the "More Microgrids Project". Its main purpose is to promote large-scale integration of distributed generation into the grid and the gradual transition from traditional grids to smart grids through the research on microgrids.

In addition to the United States, Japan, and the European Union, Canada, Australia, and other countries have also conducted research on microgrid.

China started the research of microgrid relatively late. Since 2006, microgrid technology research has been gradually included in the national ‘863’ program, ‘973’ program special funded research. China's research on microgrids is still in its infancy, but many universities, research institutes and companies are working on it.[6] Universities such as Tsinghua University, Tianjin University, and Hefei University of Technology, as well as the State Grid, Southern Power Grid and other companies are conducting research on microgrids. Relevant experimental platforms have been established.

In the application process of traditional AC microgrids or novel DC microgrids, AC/DC sources and AC/DC loads require multiple power conversions through converters, which has a negative impact on power utilization and power quality. Nanyang Technological University in Singapore proposed an AC/DC hybrid microgrid in 2010, reducing the number of repeated changes in electrical energy. The Labein microgrid of Spain and the microgrid of South China University of Technology include a DC bus which is the beginning of hybrid microgrid. The real realization of AC/DC hybrid microgrid is Japan's sendai microgrid, which contains a variety of AC/DC sources and AC/DC loads. Due to the late development of hybrid AC/DC power grids, there are few demonstration projects worldwide. The typical renewable energy laboratory in the United States includes DC buses that can run AC and DC microgrids at the same time. In China, research has been done in the related theory and engineering practice of hybrid microgrids, mainly focusing on distributed power access technology and the control of hybrid microgrid operation. South China University of Technology has established a DC microgrid test system, based on which some preliminary explorations of hybrid power grids have been made. In general, the theoretical research and engineering practice of AC/DC hybrid microgrid is at an exploratory stage.

1.2.2 Research status of microgrid control strategy

The control of microgrid can be divided into three vertical layers.[7] The first layer is the control of DGs. It is realized by the control of the interface converters. The second layer is the overall control strategy of the microgrid, which can be mainly divided into master-slave control, peer-to-peer control and integrated control. The third layer involves the coordination of the microgrid and utility grid to achieve the purpose of economic optimization. This novel mainly discusses about the first two layers of the control strategy. The third-level is not under consideration. The control strategy of DGs is the base of the overall microgrid control strategy, and the overall control strategy is achieved through the combination of the control of DGs.

1.2.2.1 Control strategy of distribute generators

The research of microgrid is based on electronic technology. DGs need to access the microgrid via electronic converters (such as DC-AC, AC-DC, and DC-DC converters). The control of DGs is achieved through the control of the converters. Literature [8] summarizes the control strategies of DC-AC, AC-DC and DC-DC converters. Literature [9] explains the theory of VF control, PQ control and droop control of the inverter based on grid-connected mode and islanding mode of AC/DC hybrid microgrid. Literature [10] proposed an adaptive droop control method for DC-DC converter to improve the accuracy of power distribution. Literature [11] proposed a segmented control strategy based on bus voltage signals to distribute the electrical energy reasonably and realize the coordination of DGs. Literature [12] clarifies the theory of VF control and PQ control, and achieves smooth switching of different operation modes. According to the different roles of DGs in the operation of the microgrid, the control strategy of DGs can be divided into voltage control and current control [13].

1.2.2.1.1 Voltage control

The DG can be equivalent to a controlled voltage source when it is under voltage control. It plays the role of supporting AC microgrid voltage, frequency or DC microgrid bus voltage. When microgrid operates in islanding mode, it must contain at least one voltage control source to provide a reference for the operation of the entire microgrid.

AC microgrid has two control targets: voltage and frequency. It is necessary to keep the voltage and frequency of the entire network stable during the operation time. AC voltage control can be divided into VF control and droop control. The goal of VF control is to make the voltage amplitude and frequency equal to the voltage reference V_{ref} and frequency reference f_{ref}. This control method mainly provides voltage and frequency support for the islanding operation of the microgrid. [14].

Droop control is a control method that simulates the primary frequency regulation and voltage regulation static characteristics of conventional synchronous generators. In AC microgrid, droop control includes (active power-frequency (P-f), reactive power-voltage (Q-U)) and (active power-voltage (P-U), reactive power-frequency (Q-f)) [14]. The choice between the two control strategies must be made according to the line parameters. For high-voltage microgrids, the inductance of the line parameters is much greater than the resistance. In this case, P-f and Q-U droop control are applied. For medium and low-voltage microgrids, the value of inductance is close to or far less than the value of resistance. In this case, P-U, Q-f droop control should be applied [15]. The following is the droop characteristic lines of the traditional high-voltage system as an example.

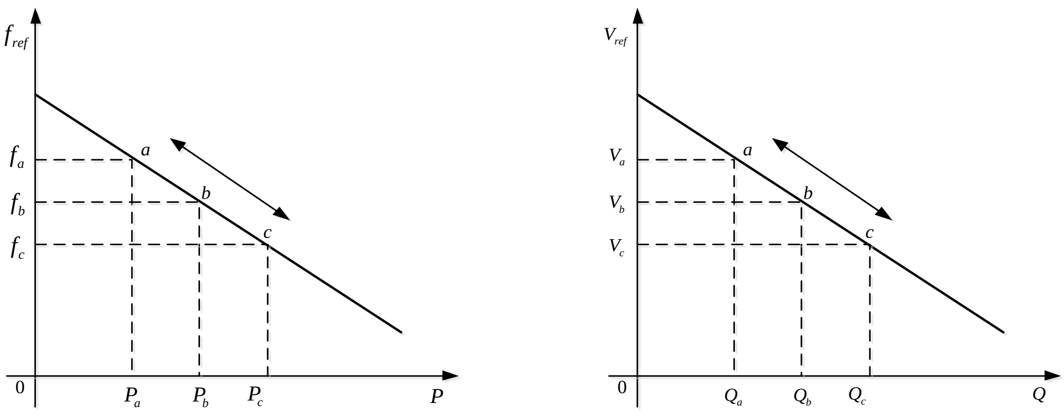

(a) P-f droop characteristic line.

(b) Q-U droop characteristic line.

Figure 1- 2 Droop characteristic lines in HV system.

As shown in Figure 1-2, the Y-axis corresponds to frequency reference f_{ref} and the voltage reference V_{ref}. The X-axis corresponds to output active power and reactive power. The working point of inverter moves along the characteristic line according to the output active and reactive power. The output frequency reference f_{ref} and voltage reference V_{ref} are determined according to the characteristic line. When output active power or reactive power of inverter increases, the working point moves downwards in the direction of b-c, and the reference voltage or frequency of the system decreases from the rated value. Conversely, when output active power or reactive power of inverter decreases, the working point moves upward in the direction of b-a. The reference voltage or frequency of the system increases over the rated value. It can be seen that the droop control is a kind of differential control, and the output reference value of the droop controller will change with the change of working status.

The control of DC microgrid is simpler than that of AC microgrid. Compared with AC microgrid, which requires to keep both AC voltage and the frequency under control, DC microgrid only needs to pay attention to DC voltage. During the operation of DC microgrid, it is necessary to ensure that DC bus voltage is stable. DC voltage control strategy can be divided into constant voltage control and droop control. The purpose of constant voltage control is to provide rated voltage for the entire network so that other components can work properly under this reference. Constant voltage control is often used in systems where only one DG provides voltage support.

If there are two or more than two DGs in the microgrid to provide voltage reference, it is necessary to apply droop control strategy. Otherwise, current circulation may occur among DGs. Different from the droop control in AC system, in DC microgrid, droop control only has the P-U droop characteristic line. It is shown in Fig 1-3.

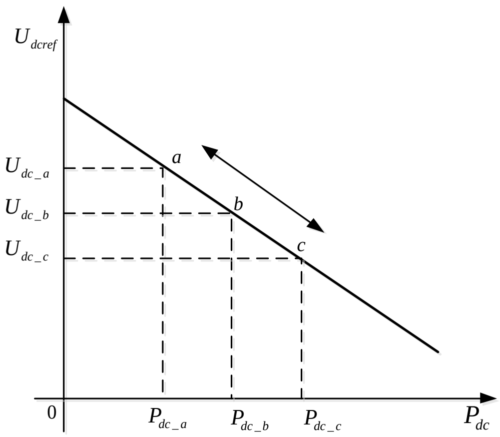

Figure 1- 3 P-U droop characteristic line.

In Figure 1-3, the Y-axis corresponds to the voltage reference and the X-axis corresponds to the output active power. Similar to the droop control of AC system, the working point moves along the droop characteristic line. Its output power reference P_{ref} is determined by the droop characteristic line. When the output active power increases, the working point moves down in b-c direction; conversely, when the output active power decreases, the working point moves up in b-a direction.

1.2.2.1.2 Current control

The DG can be equivalent to a controlled current source when it is under current control. The current control is mainly constant power control. It aims to control the DG output active power and reactive power to be equal to its reference values P_{ref} and Q_{ref} [15]. DGs under constant power control cannot provide voltage support for the microgrid. Only if the voltage amplitude and frequency of the microgrid are stable, DGs can work properly under constant power control.

1.2.2.2 Control strategy of the whole microgrid

The overall microgrid control strategy is one of the key technologies for microgrid operation. The main goal of the overall control strategy of the microgrid is to take the energy flow under control through the coordinated of DGs and loads within the microgrid so that the load can be reasonably shared among the various power supplies. As a result, the micro grid can work stably in amplitude and frequency range. [7][13][16][17] When working in grid-connected mode, the microgrid is supported by the utility grid. The control of the microgrid is relatively easy. When working in islanding mode, the microgrid is disconnected from the utility grid so the microgrid must be provided with voltage and frequency support from the internal DGs. The control strategy is relatively complex. Therefore, the control strategy in islanding mode is one of the keys of the research.

When it works in islanding mode, the microgrid is provided with voltage and frequency references by internal DGs. According to different voltage and frequency control methods, the overall control strategy of microgrid can be divided into centralized control and decentralized control [7].

1.2.2.2.1 Master-slave control

In master-slave control, a DG must be chosen as the master source to provide voltage and frequency reference (only voltage reference in DC microgrid) to the whole system. Usually the master source works under VF control (constant voltage control in DC microgrid) and the rest of the DGs work under power control to provide power to the system. The master source is usually controllable such as fuel cell, gas turbine, diesel generator, or energy storage device. Intermittent DGs such as PVs, wind turbines, etc. often work as slave sources due to their instability. Literature [18] gives a detailed introduction to the control loop of master-slave control and implements simulation of master-slave control based on

PSCAD. Literature [19] applies master-slave control strategy in microgrid. It points out that when the master source capacity is insufficient to suppress the power fluctuation, the microgrid will not be able to operate stably. Literature [20] proposed a multi-master-slave control strategy that combines master-slave control and droop control. It solves the problem of the requirement of large master source capacity in master-slave control. Literature [21] applies several DGs with peer-to-peer control as the main power supply during the operation of the microgrid to raise stability. The capacity of the master source is also increased at the same time. When master-slave control is applied, the master source is responsible for the power balance in microgrid. Power fluctuation in microgrid is suppressed by the master source, so the stability of microgrid depends highly on the master source. Therefore, the capacity of master source must be large enough to ensure the reliability. When master-slave control is applied, the status of master source is equivalent to the utility grid. However, since the master source capacity is much smaller than the utility grid, the operating reliability is not high. Therefore, when the master source fails or its capacity is insufficient to suppress power fluctuations, faults may occur.

1.2.2.2.2 Peer-to-peer control

Peer-to-peer control [22] refers to that all DGs in microgrid work under droop control to participate in voltage and frequency adjustment. Peer-to-peer control is a decentralized control method in which DGs are controlled only by local information. When power fluctuations occur in microgrid, DGs share the corresponding change according to the respective droop characteristic lines. In this way, it can realize “plug and play” of DGs and loads. There is no master source and slave source and all DGs share the same status. The peer-to-peer control strategy based on droop control is a kind of differential control strategy. The reference value will change according to different situation. The problem of load sharing is a major problem in peer-to-peer control and can be improved by increasing the droop coefficient. However, the increase in the droop coefficient will in turn lead to an increase in the voltage deviation. As a result, a balance must be found between the two. Literature [23] points out that due to the influence of transmission line, the power cannot be reasonably distributed among the DGs. Current circuit flow occur among DGs which will lead to extra power loss. In literature [24][25], a controller with self-adaptive adjustment of droop coefficient is proposed based on the traditional droop control strategy, so as to achieve small offset. Literature [26][27] makes a comparison between high-voltage system and low-voltage system and made a modification to the traditional P-f, Q-V droop characteristics. It obtains good operation behaviour.

Compared to master-slave control, peer-to-peer control applies multiple DGs to maintain power balance control at the same time. When some DG fails, it will not affect the operation of the entire microgrid which leads to a higher reliability.

Till now, a great deal of research has been conducted on the control strategy of AC and DC microgrids. Some control strategies have been applied to AC microgrids and got good results. The structure of AC/DC hybrid microgrid is more complex. As a result, its control strategy is more complex. More researches are required to be done on the control strategy of AC/DC hybrid microgrid.

1.3 Summary

The present control strategy applied to AC/DC hybrid microgrid is not yet mature and theoretical research is absent. This paper focuses on the control strategy of AC/DC hybrid micro-grid. The main contents include:

1) Based on the background of a small plant, an AC/DC hybrid microgrid structure including a photovoltaic power source, a fuel cell, energy storage devices, AC and DC loads are proposed. Based on PSCAD/EMTDC simulation software, the electromagnetic transient simulation models of DGs and their interface converter are established.

2) Different control strategies are proposed based on different operating modes of AC/DC hybrid microgrids. The control strategies of AC sub-network and DC sub-network are studied. This paper focuses on a control strategy based on the entire network of AC-DC mixed islanding mode. This control strategy has no restrictions on the capacity of the AC and the DC sub-networks and realizes the plug and play of DGs.

3) The smooth transition between grid-connected mode and islanding mode is studied. By analysing the control loop framework, the reason for transition impacts is explained. A new type of smooth transition method based on islanding signal is proposed and the comparison between the traditional smooth transition method is made. Finally, based on the new smooth transition method, the influence of load on smooth transition is also studied.

4) Simulation based on PSCAD/EMTDC software to verify the effectiveness of the control strategy in different modes and smooth transition method is conducted.

2 MODELING OF HYBRID MICROGRID BASED ON A SMALL PLANT

2.1 Hybrid microgrid structure of a small plant

In this paper, an AC/DC hybrid microgrid model of a small plant consists of PV panel, fuel cell, batteries, AC and DC loads is built. The AC/DC hybrid microgrid in this paper has the following features. Firstly, the capacity of the microgrid is around several kilowatts. Secondly, the small plant contains a large number of frequency conversion devices which can be connected to DC bus directly to avoid redundant power conversion. Here we assume that the capacity of DC and AC sub-networks are similar. Thirdly, the plant area is relatively large. The length of the transmission lines between DGs and loads are about hundreds of meters. The impedance of transmission line cannot be neglected.

This novel investigates a small factory in southern part of Jiangsu Province, China. The maximum load of the system is about 300kW. The traditional AC load still dominates. However, with the increasing popularity of mobile phones, computers, and electric vehicles, the DC load is increasing. As a result, the amount of AC and DC loads will become more and more balanced. As mentioned before, the frequency transfer equipment can also be treated as DC loads. Therefore, we assume that the amount of AC and DC load is approximately equal to discuss about the control strategy of AC/DC hybrid microgrid in which AC sub-network and DC sub-network share similar capacity.

Based on the above analysis, a small factory AC/DC hybrid microgrid structure with photovoltaic power supply, fuel cell, battery storage, AC load, and DC load can be obtained, as shown in Fig 2-1.

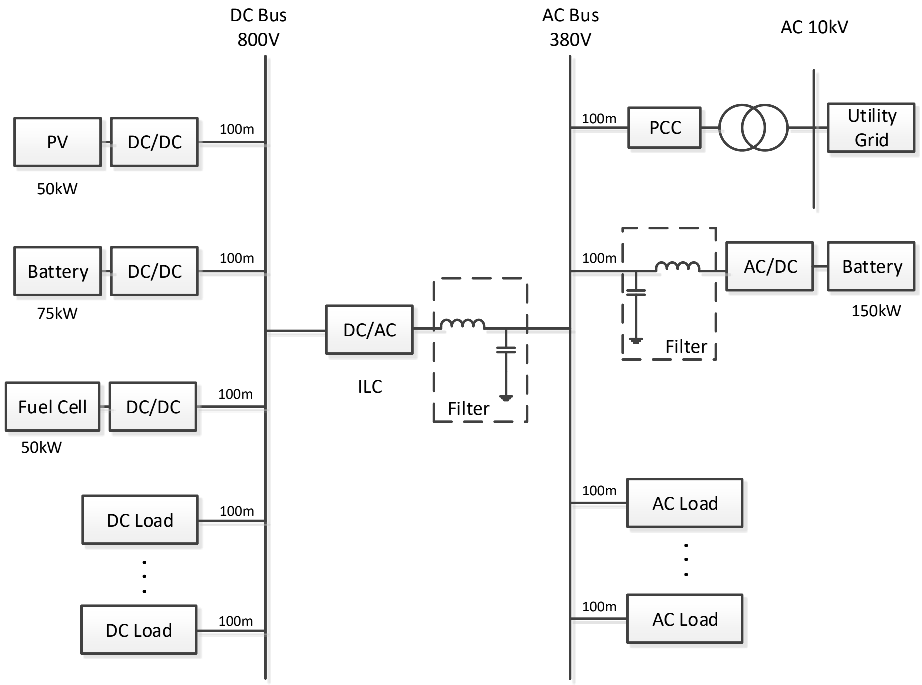

Figure 2- 1 Hybrid microgrid structure of a small plant.

In Fig 2-1, the hybrid microgrid of a small plant consists of three parts: AC sub-network, DC sub-network and interlink converter(ILC). The AC sub-network is directly connected to the utility grid through point of common coupling (PCC) while the DC sub-network is connected to the AC sub-network through ILC. AC transmission line resistance r=0.5Ω/km, inductive reactance x=0.073Ω/km. DC transmission line resistance r=0.325Ω/km.

In order to maximize the use of renewable energy, PV panels are erected on the roof of the plant. In general, taking into account the complex factors such as natural shelter and area utilization, the 1 kW occupied roof area is about 15 to 20 square meters. The plant area is about 1000m^2, so the PV capacity is about 50kW. Fuel cell is a controllable power supply, which is used to ensure continuous supply of important loads under special operating conditions with a capacity of 50 kW. The capacity of the battery in DC sub-network and AC sub-network are 75kW and 150KW respectively to ensure continuous supply of all loads during a certain period of time during island operations, while suppressing the impact of distributed power and load fluctuations in the microgrid system. The AC bus has a rated voltage of 380V and a frequency of 50Hz, so the AC sub-network can be connected directly to the utility grid. A unified standard of DC bus voltage value has not been reached yet. In the literature, the DC bus voltage is selected between 600V to 3.5kV [13-17]. In this novel, the rated voltage of DC bus is selected as 800V.

2.2 Modelling of distributed generators and converters

As shown in Fig. 2-1, the AC/DC hybrid microgrid contains DGs such as PV, fuel cell and batteries. All DGs need to be connected to the microgrid through converters and the control of each DG is implemented by the control of converters. The following paragraph briefly analyzes the theory and control strategies of each DG and its interface converter.

2.2.1 Photovoltaic cell

2.2.1.1 Modelling of Photovoltaic cell

Photovoltaic cell is a semiconductor device that uses photovoltaic effect to convert solar energy into electrical energy [33]. The equivalent circuit of the photovoltaic cell is shown in Fig 2-2.

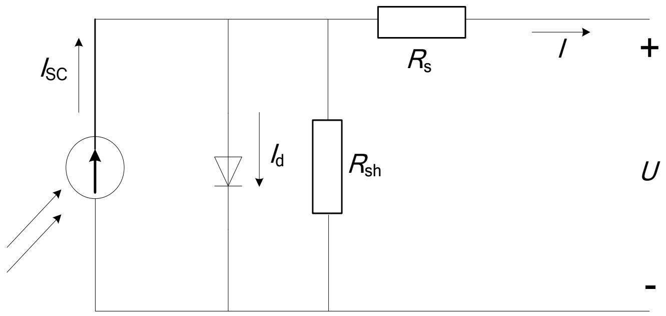

Figure 2- 2 Photovoltaic cell equivalent circuit model.

In Fig.2-2, I_{SC} is photon excitation current in photovoltaic cell. Id is total diffusion current through the PN junction. R_{sh} is the bypass resistance, which is usually large and can be ignored in the calculation. The series resistance R_s is mainly composed of the body resistance of the battery, the resistance of the electrode conductor, the surface resistance, and the contact resistance between the electrode and the silicon surface. Photovoltaic cell external characteristic mathematical model is shown as follows:

$$I = I_{SC} - I_0 \left(\exp\left(\frac{U + I \cdot R_s}{n \cdot V_T} \right) - 1 \right) \tag{2-1}$$

2.2.1.2 Modelling of photovoltaic cell’s interface converter

Boost chopper circuit (Boost circuit) is usually applied to PV, the structure is shown in Figure 2-3.

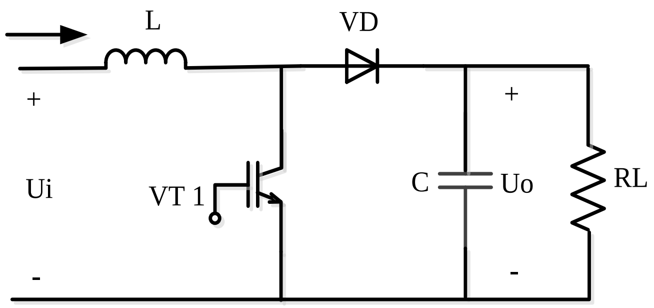

Figure 2- 3 Structure of boost circuit.

The theory of the boost chopper circuit is described in [34]. By controlling the duty cycle of the VT1 switching signal, DC-DC power transmission is implemented. It should be noted that the output voltage U_o should be greater than the input voltage U_i in boost circuit, otherwise the energy will fail to be transmitted. Boost circuit is a one-way DC-DC circuit. The power can only be transmitted from low voltage side to high voltage side.

Usually, the converter of PV is boost chopper circuit, which is mainly responsible for implementing MPPT control of PV. The control structure is shown in Figure 2-4.

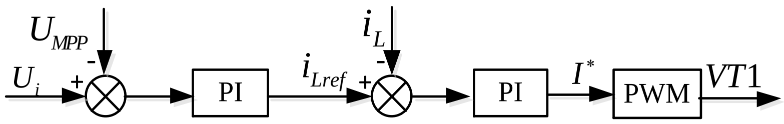

Figure 2- 4 MPPT control structure of boost circuit.

In Fig 2-4, U_i and U_{MPP} refer to the output voltage of PV and maximum power point voltage respectively. i_L and i_{Lref} refer to the measured inductor current and reference current value respectively. VT1 is the output converter control signal. In addition, under certain extreme conditions (such as when the power in the microgrid is seriously excessive), the converter should also be able to reduce the output power.

In order to verify the photovoltaic power supply model, simulation is implemented with the change of light intensity. The simulation result is shown in Figure 2-5.

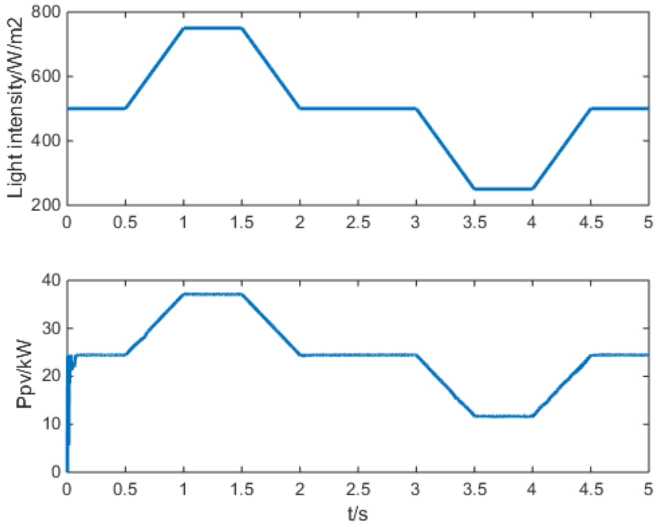

Figure 2- 5 Light intensity and PV output power.

The standard operating condition of this photovoltaic cell model is 1000 W/m^2 and 25°C. With the same temperature condition, the light intensity is changed, as shown in Fig 2-5. The output power of the PV panel can reflect the changes of light intensity correctly.

2.2.2 Fuel cell

2.2.2.1 Modelling of fuel cell

Fuel cell is a power generation device that directly converts chemical energy into electrical energy through electrochemical reaction. Fuel cell has a high energy conversion rate and low pollutant emissions. Depending on the type of internal electrolyte, fuel cells can be divided into proton exchange membrane fuel cells (PEMFC), phosphoric acid fuel cells (PAFC), alkaline fuel cells (AFC), solid oxide fuel cells (SOFC), molten carbonate fuel cells(MCFC), etc. [35][36].

The proton exchange membrane fuel cell structure [51] is shown in Fig. 2-6. Its main components include membrane electrode assemblies, bipolar plates and sealing components. The membrane electrode assembly consists of a cathode-anode porous gas diffusion electrode and an electrolyte membrane. It is the core component of the fuel cell. The cathode and the anode on both sides of the electrolyte membrane are oxidized and reduced respectively. The electrons work through the external circuit and the reactant is water.

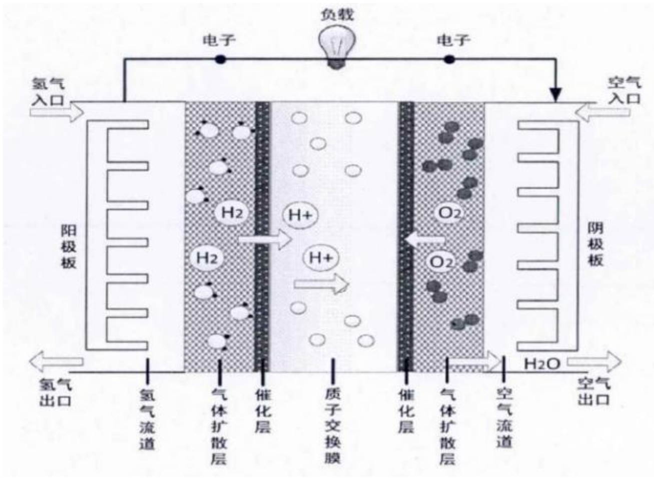

Figure 2- 6 Structrure diagram of fuel cell.

The conversion efficiency of fuel cell is high, usually from 45% to 60% [37], and it can maintain high efficiency regardless of load level. In addition, the fuel cell has a fast load response and can switch from the lowest power to the rated power in several seconds. In practical applications, the cells are usually formed in parallel to form a fuel cell stack.

The equivalent circuit in steady state is shown in Fig 2-7.

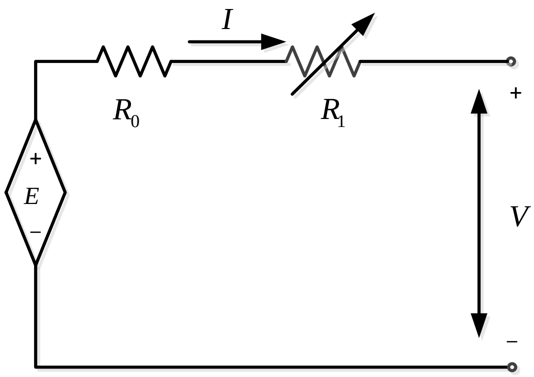

Figure 2- 7 PEMFC equivalent circuit.

In Fig. 2-7, E is the equivalent electromotive force of the fuel cell, which is determined by the standard electromotive force of the fuel cell under standard conditions, the operating temperature of the fuel cell, the gas pressure of the fuel and oxidant. R_0 is the ohmic resistance of the fuel cell. R1 is the equivalent internal resistance of electrochemical polarization and concentration polarization of the fuel cell, which is a function of pressure, temperature, and output current.

2.2.2.2 Modelling of fuel cell's interface converter

Boost chopper circuit is also applied to fuel cell as converter to transfer power. The control strategy mainly includes constant DC voltage control and droop control. The control structures are shown in Fig 2-8 and Fig 2-9.

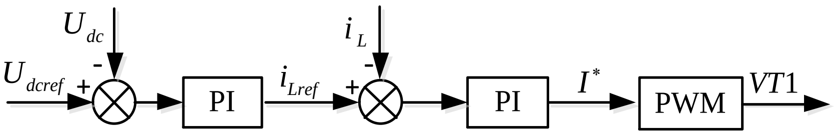

Figure 2- 8 Constant DC voltage control structure of boost circuit.

In Fig. 2-8， U_{dcref} and U_{dc} refer to DC bus voltage reference and measured DC bus voltage. i_{Lref} and i_L refer to current reference and measured current of inductor. VT1 is control signal of the converter.

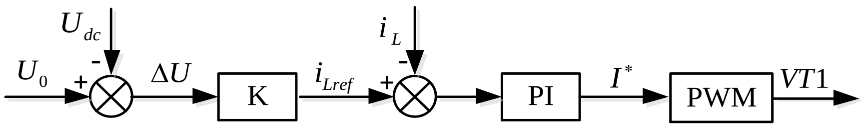

Figure 2- 9 Droop control structure of boost circuit.

In Fig. 2-9, U_0 and U_{dc} refer to DC bus voltage reference and measured value. K is the droop coefficient.

To verify the correctness of fuel cell and its converter, the following simulation is completed. The fuel cell works in constant DC bus voltage control mode to maintain the DC bus equal to 800V. When t=0, the required power is 10kW. When t=1s, t=2s, t=3s, the load increases 10kW, 10kW and 20kW respectively. When t=4s, the load decreases 40kW. In this process, the output power of the fuel cell and the DC bus voltage is shown in Figure 2-10.

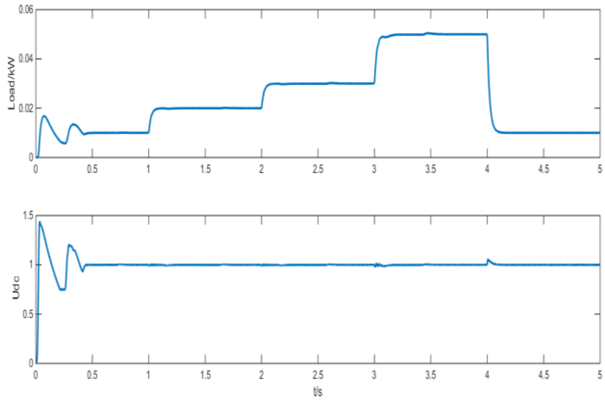

Figure 2- 10 Fuel cell output power and DC bus voltage.

It can be seen from the figure that when the fuel cell works in constant voltage control mode, it can suppress the load fluctuation and maintain the DC bus voltage well. The voltage has only small disturbances when load changes and the disturbances are within the allowed range.

2.2.3 Battery

2.2.3.1 Modelling of battery

Battery is one of the most important components of microgrid and takes responsibility for maintaining the stability of microgrid. The energy storage system in microgrid can be divided into 'power type' and 'energy type' based on its output characteristics [38-41]. The 'power type' energy storage device (such as super capacitor) has a fast response speed and high charge and discharge power, but its capacity is relatively small and the cost is high. 'Energy-type' energy storage device (such as battery) has a slower response speed, but it has much larger capacity. Battery is inexpensive, and easy to maintain. Therefore, it is widely used in microgrids. According to different internal chemical reaction materials, batteries can be divided into lead-acid battery, lithium battery, nickel-metal hydride battery, etc. Among them, lead-acid battery is the most widely used.

The electrolyte of lead-acid batteries is dilute sulfuric acid, and its internal redox reaction is reversible. Therefore, lead-acid batteries can be repeatedly charged and discharged. The specific working theory is shown in [37]. The common equivalent circuit models for battery are universal model, third-order dynamic model and fourth-order dynamic model [37].

As shown in Figure 2-11, the external characteristics of the battery show a strong non-linearity, and a general model of the battery can be obtained by approximately fitting the terminal voltage curve when the battery is discharged, as shown in Figure 2-12. The general model of the battery consists of a controlled voltage source in series with a fixed resistor.

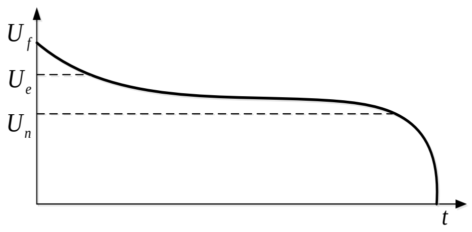

Figure 2- 11 Battery discharge terminal voltage.

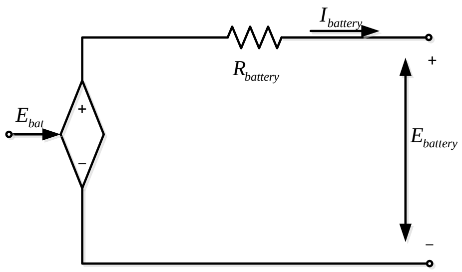

Figure 2- 12 Equivalent circuit of battery.

The two most important parameters that show the state of the battery are the terminal voltage $E_{battery}$ and the state of charge SOC, as shown in Equation (2-2) and Equation (2-3).

$$\begin{aligned} E_{battery} &= E_{bat} - R_{battery} I_{battery} \\ &= E_0 - K\left(\frac{Q}{Q - \int I_{battery} dt}\right) + A \cdot \exp(-B\int I_{battery} dt) - R_{battery} I_{battery} \end{aligned} \tag{2-2}$$

$$SOC_t = SOC_{t_0} - \frac{1}{Q}\int_{t_0}^{t} \eta I_{battery} dt \tag{2-3}$$

The references and units of each parameter in the formula are shown in Table 2-1:

Table 2- 1 Battery model parameters.

Parameter	Meaning	Parameter	Meaning
$E_{battery}$（V）	Terminal voltage	E_{bat}（V）	No-load voltage
$R_{battery}$（Ω）	Equivalent internal impedance	$I_{battery}$（A）	Charge and discharge current
E_0（V）	Stantard voltage	K（V）	Polarization voltage
Q（Ah）	Battery capacity	A（V）	Index domain voltage drop
B（Ah^{-1}）	Inverse of the exponent domain time constant	SOC_t	State of charge at t
SOC_{t0}	State of charge at t_0	η（%）	Charge and discharge efficiency

2.2.3.2 Modelling of battery's interface converter

The interface converter of the battery must allow the two-way flow of energy. Therefore, a current-reversible chopper circuit (buck-boost circuit) is usually applied. The structure is shown in Fig. 2-13.

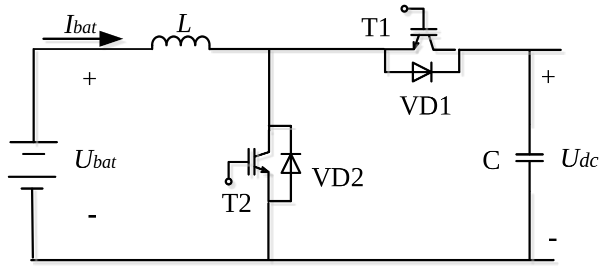

Figure 2- 13 Bidirectional DC-DC circuit structure.

By controlling the on-off of T1 and T2, the bi-directional DC-DC converter can operate in step-up or step-down mode. The specific working theory is shown in literature [34]. The common control of the bi-directional DC-DC converter include constant DC voltage control, droop control and constant power control. The control structures are shown in Fig. 2-14, Fig. 2-15 and Fig. 2-16. Double-loop control strategy is usually applied in bi-directional DC-DC converters. The outer-loop regulator is responsible for achieving the control target and providing current reference for the inner-loop regulator. The inner-loop regulator is used to improve the dynamic response of the system.

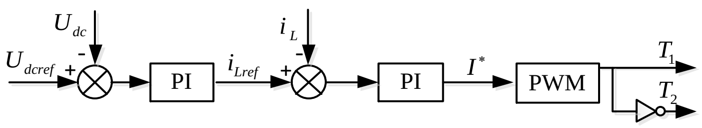

Figure 2- 14 Constant DC voltage control structure of buck- boost circuit.

In Fig 2-14, U_{dcref} and Udc are reference value and measured value of DC bus. i_L and i_{Lref} are measured value and reference value of the inductor current respectively. T1 and T2 are control signal of the converter.

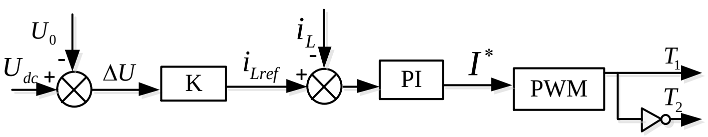

Figure 2- 15 Droop control structure of buck- boost circuit.

In Fig 2-15, U_0 and U_{dc} are the DC bus voltage reference value and measured value. K is the droop coefficient.

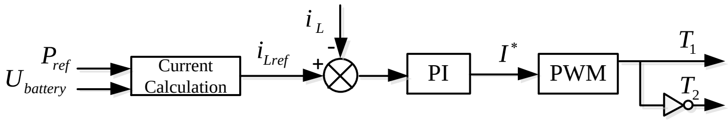

Figure 2- 16 Constant power control structure of buck- boost circuit.

In Fig 2-16, P_{ref} and $U_{battery}$ are the output power reference and voltage of the battery, respectively.

In order to verify the model of battery and its converter, constant voltage control and power control are applied. First, the charge and discharge process of battery power control is simulated. Assuming that the initial SOC value is 0.6, t=0-1s, the battery discharges with a constant power of 30kW. t=1-3s, the battery is charged with a constant power of 60kW. t=3-5s, the reference value of the power outer-loop is 0. The value of charge and discharge power, output voltage and SOC change as shown in Figure 2-17.

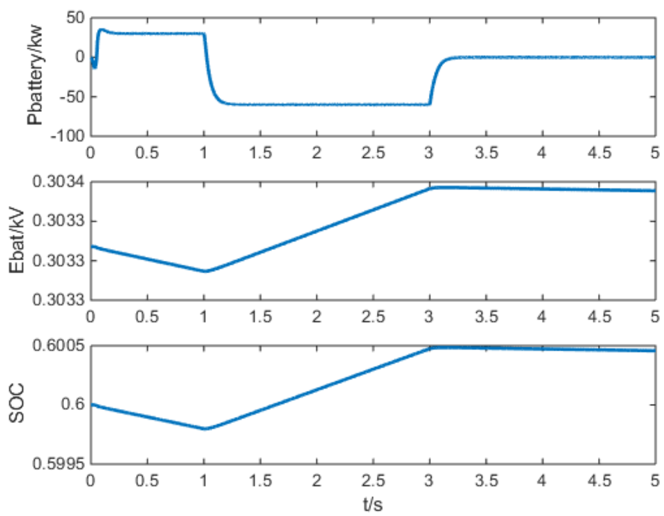

Figure 2- 17 Output power, no-load voltage and state of charge of battery.

From Fig 2-17, it can be seen that the battery can work under constant power charge and discharge control according to the given power. The output voltage and SOC of the battery will change according to the charging and discharging process and the change trend is same.

Following is the verification of the constant voltage control strategy. DC bus voltage reference value is 800V. When t=0, the load is 20kW. It increases 40kW at t=1s and decreases 20kW at t=3s. During this process, the output power of battery and DC bus voltage are shown in Fig 2-18.

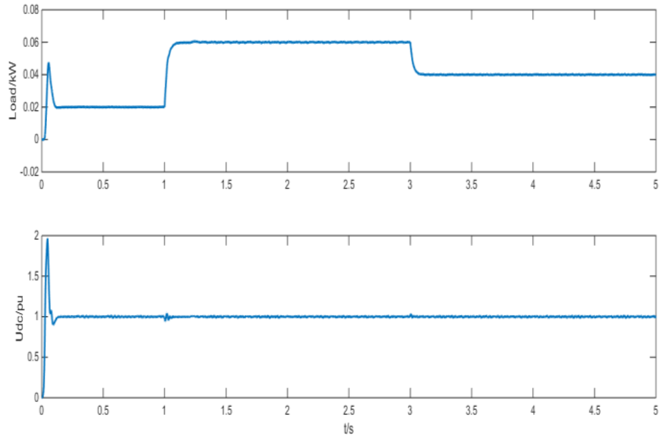

Figure 2- 18 Load and DC bus voltage value.

Similar to the constant voltage control mode of the fuel cell, when battery works in this mode. it can quickly respond to the load fluctuation within allowed range and maintain the stability of the DC bus voltage.

2.3 AC-DC converter

2.3.1 AC-DC converter control theory

AC-DC converter is the channel for AC and DC sub-network power flow and it is one of the most important components of the AC/DC hybrid microgrid. The structure of AC-DC converter is shown in Fig 2-19.

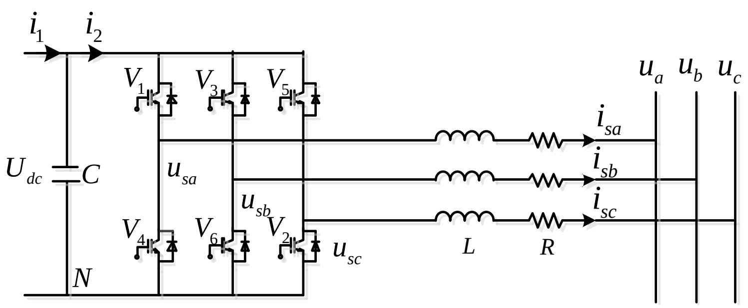

Figure 2- 19 Structure of AC-DC converter.

AC voltage equation can be described as [42]:

$$\begin{cases} s_q U_{dc} = Ri_{\mathrm{d}} + L\dfrac{\mathrm{d}i_{\mathrm{d}}}{\mathrm{d}t} - \omega L i_{\mathrm{q}} + u_{\mathrm{d}} \\ s_d U_{dc} = Ri_{\mathrm{q}} + L\dfrac{\mathrm{d}i_{\mathrm{q}}}{\mathrm{d}t} + \omega L i_{\mathrm{d}} + u_{\mathrm{q}} \end{cases} \tag{2-4}$$

U_{dc} is the DC-side voltage of the AC-DC converter. s_d and s_q refer to direct and quadrature axis components of the switching function. L and R are filter inductance and resistance respectively. i_d, u_d, i_q, and u_q refer to the direct and quadrature axis voltages and currents on AC side of AC-DC converter respectively. ω is angular frequency of the grid.

DC voltage equation:

$$C\frac{dU_{dc}}{dt} = i_1 - \frac{3}{2}(i_d s_d + i_q s_q) \tag{2-5}$$

C is the DC-side capacitance of the AC-DC converter.

Power equation:

$$\begin{cases} P = \dfrac{3}{2}(u_{\mathrm{d}} i_{\mathrm{d}} + u_{\mathrm{q}} i_{\mathrm{q}}) \\ Q = \dfrac{3}{2}(u_{\mathrm{q}} i_{\mathrm{d}} - u_{\mathrm{d}} i_{\mathrm{q}}) \end{cases} \tag{2-6}$$

The d-axis of the synchronous rotating coordinate system is oriented in the direction of the grid voltage space vector. The AC-DC converter mathematical model based on grid voltage orientation can be obtained:

$$\begin{cases} u_{\mathrm{sd}} = Ri_{\mathrm{d}} + L\dfrac{\mathrm{d}i_{\mathrm{d}}}{\mathrm{d}t} - \omega L i_{\mathrm{q}} + u_{\mathrm{d}} \\ u_{\mathrm{sq}} = Ri_{\mathrm{q}} + L\dfrac{\mathrm{d}i_{\mathrm{q}}}{\mathrm{d}t} + \omega L i_{\mathrm{d}} \end{cases} \tag{2-7}$$

$$\begin{cases} P = \dfrac{3}{2} u_{\mathrm{d}} i_{\mathrm{d}} \\ Q = -\dfrac{3}{2} u_{\mathrm{d}} i_{\mathrm{q}} \end{cases} \tag{2-8}$$

From Equation (2-8), it can be seen that AC-DC converter AC side active power is only related to the direct axis current i_d and reactive power is only related to the quadrature axis current i_q. Therefore, independent adjustment of i_d and i_q can be made to realize decoupling of active and reactive power.

2.3.2 AC-DC converter control strategy

AC-DC converter control strategy can usually be divided into DC voltage control, VF control and power control.

2.3.2.1 DC voltage control

In grid-connected mode, DC voltage control [43] is usually applied to suppress power fluctuation in DC sub-network so that the DC bus voltage can maintain the reference value. The control structure of DC voltage control is shown in Fig. 2-20.

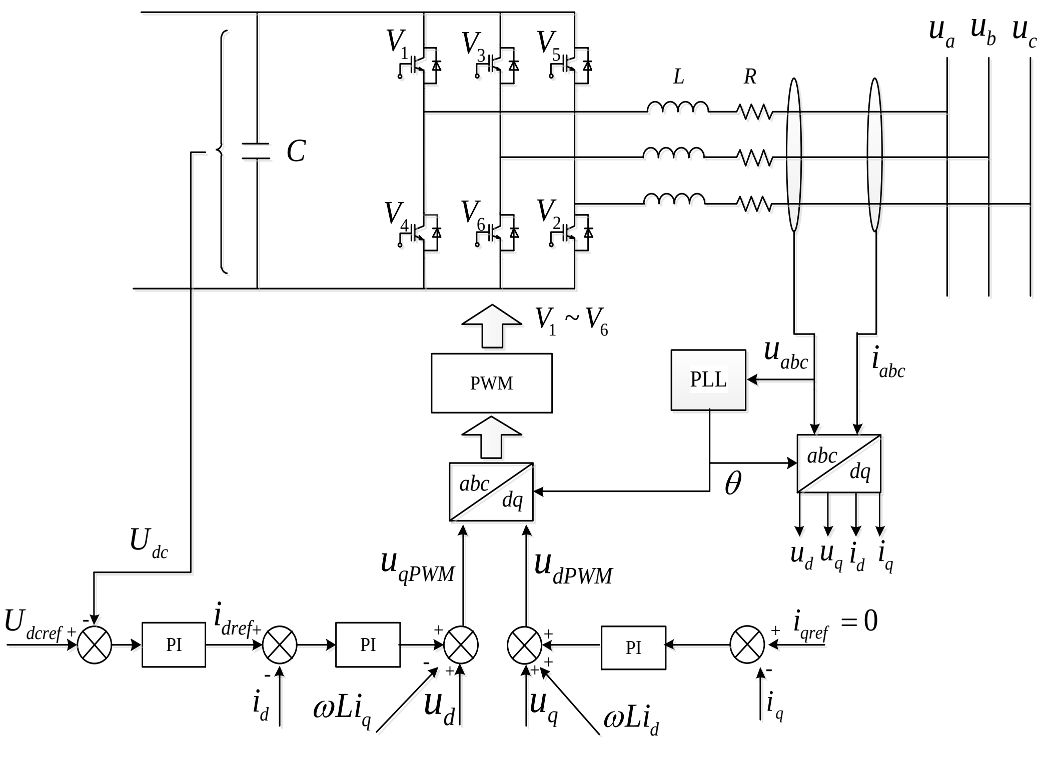

Figure 2- 20 AC-DC Converter DC Voltage Control Structure.

In Fig 2-20, L and R refer to filter inductance and resistance. PLL is a phase-locked loop. U_{dcref} and U_{dc} refer to reference and measured values of DC voltage. i_d, i_q, i_{dref}, i_{qref} are reference and measured value of AC current. u_{dPWM} and u_{qPWM} refer to PWM modulation wave. V1 ~ V6 are control signals of AC-DC converter.

In order to verify DC voltage control, simulation is performed. When t=0s, DC load is 20kW. When t=1s and t=2s, DC load increases 10kW and 20kW respectively. When t=3s, DC load reduces 40kW. The active and reactive power output of AC-DC converter is shown in Figure 2-21.

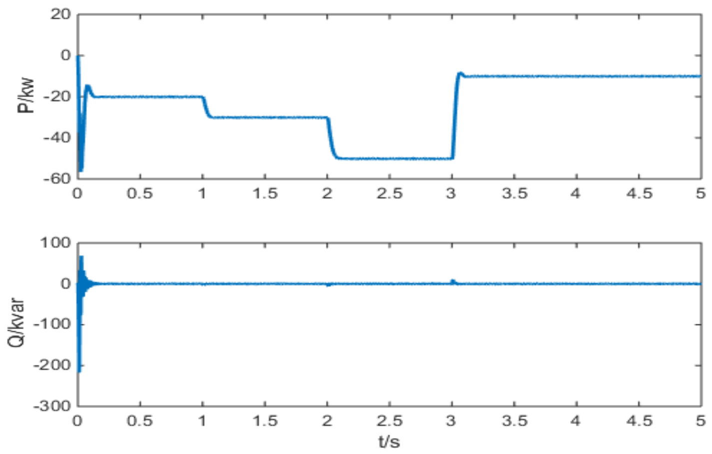

Figure 2- 21 AC-DC converter active and reactive transmission power.

The direct and quadrature axis components of AC current and DC voltage are shown in Fig 2-22.

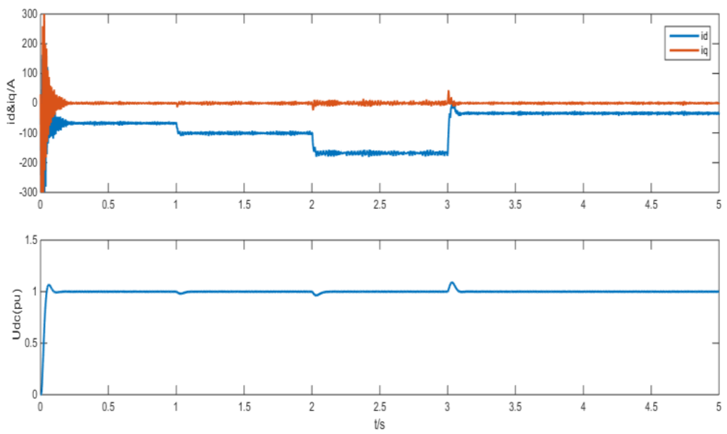

Figure 2- 22 AC-DC converter d-axis current, q-axis current, DC voltage.

In Fig. 2-22, it can be seen that the in AC side. Direct and quadrature axis current correspond to active and reactive power respectively, realizing the decoupling of active and reactive power. The DC bus voltage will fluctuate slightly with the change of load, but it can quickly recover to the rated voltage, and the voltage fluctuation value is within the acceptable range.

2.3.2.2 VF control

In islanding mode, VF control [43] is usually applied to AC-DC converter to provide voltage and frequency support for AC sub-network. The control structure is shown in Figure 2-23.

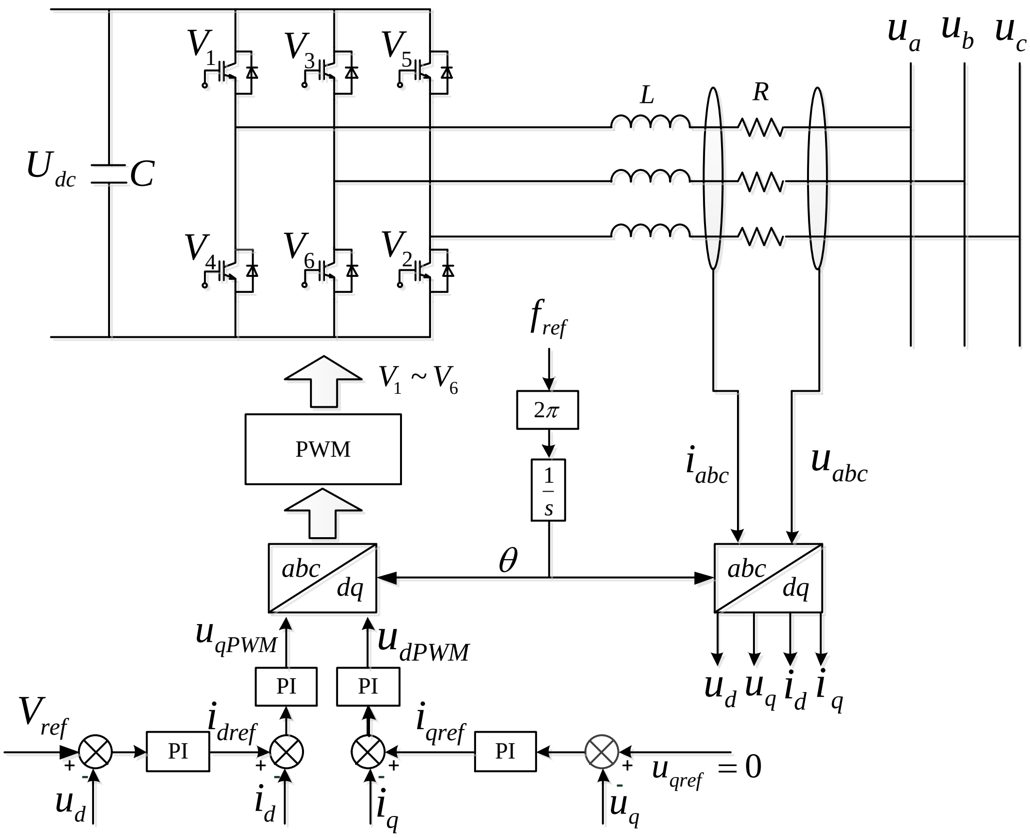

Figure 2- 23 AC-DC converter VF control structure.

In Figure 2-23, u_{dref}, u_{qref}, u_d, u_q are reference and measured value of direct axis and quadrature axis of AC voltage. i_d, i_q, i_{dref}, i_{qref} are reference and measured value of direct axis and quadrature axis of AC current. f_{ref} is the frequency reference. u_{dPWM} and u_{qPWM} are direct axis and quadrature axis PWM modulation wave.

In order to verify the reliably of VF control, simulation is performed. When t=0s, AC load is 20kW. When t=1s and t=2s, DC load increases 10kW and 20kW respectively. When t=3s, DC load reduces 30kW. AC-DC converter AC voltage, current and its direct axis and quadrature axis components, active and reactive power, respectively are shown in Figure 2-24 and Figure 2-25.

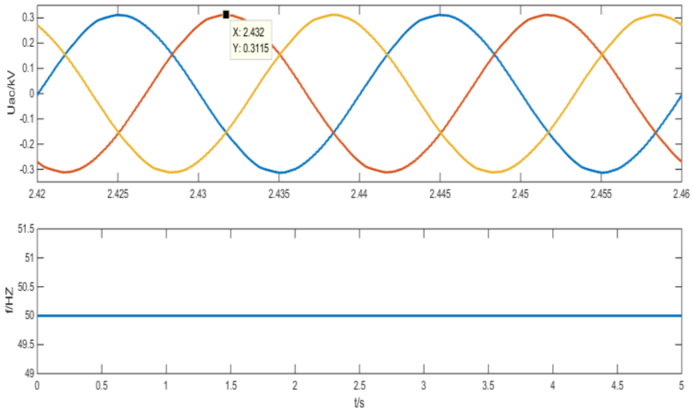

Figure 2- 24 AC voltage and frequency.

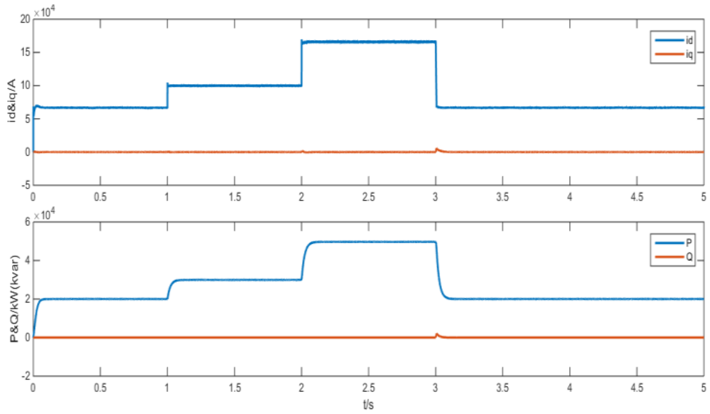

Figure 2- 25 AC-DC converter transmission current and power in VF control.

When VF control is applied, a stable 220V three-phase AC voltage can be obtained. The peak voltage is about 311V. The active and reactive power are decoupled and correspond to direct axis and quadrature axis current.

2.3.2.3 Power control

Power control can be applied in addition to the previous two control strategies. The control structure is shown in Figure 2-26.

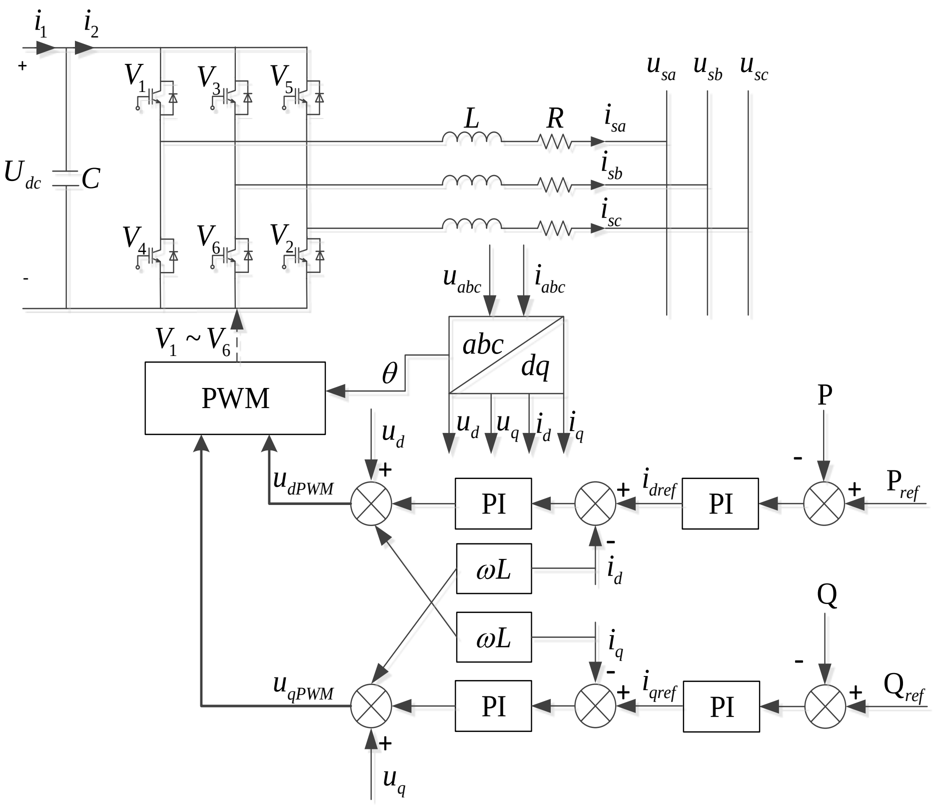

Figure 2- 26 AC-DC converter power control structure.

In order to verify power control, simulation is performed. Assume power flow from DC side to AC side is positive. When t =0s, the reference power is 20kW. When t =1.5s, the reference power becomes -30kW. When t =3s, the reference power becomes 10kW. Direct axis and quadrature axis current, transmission power are shown in Figure 2-27.

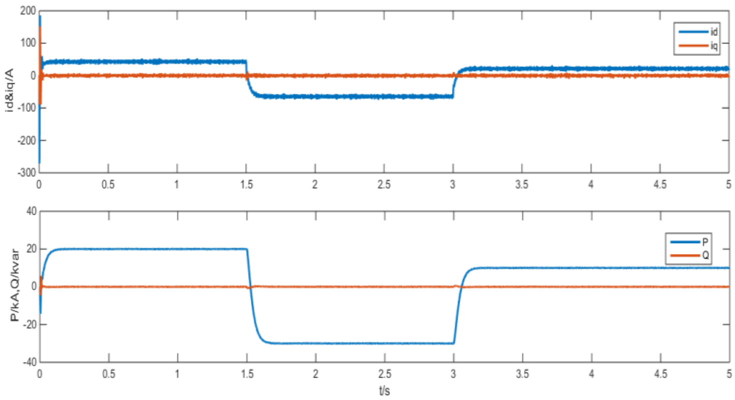

Figure 2- 27 AC-DC converter transmission current and power in power control.

2.4 Summary

In this chapter, an AC/DC hybrid microgrid structure is designed based on a small plant, preparing for the study of control methods and smooth switching. The theory and control strategy of photovoltaic cell, fuel cell, battery and the interface converters are explained. Based on PSCAD/EMTDC, the DGs and converter models are analysed. Simulation verification was is carried out and the results showed that the established models and their converter control modes can operate successfully according to the strategy.

3 HYBRID MICROGRID CONTROL STATEGY OF ISLANDING AND GRID-CONNECTED MODES

AC/DC hybrid microgrid is an effective way to integrate AC/DC distributed generators, energy storage systems and loads to improve energy utilization. Hybrid microgrid can be mainly divided into three parts: DC sub-network, AC sub-network and interconnected converter (ILC). The structure is more complex than the traditional AC micro-grid and new DC micro-grid, and the operation mode is more flexible.

Due to the complex structure of hybrid microgrid, the operation becomes more flexible and the control becomes more difficult. The control strategy is a key issue of hybrid microgrid. Literature [9] doesn't change control strategy in islanding mode. DC voltage control is still applied to ILC. In this way the fluctuation during transition can be reduced a lot. However, the control strategy requires the capacity of DC sub-network to be small. Literature [10] calculates the power to be exchanged through AC-DC converter, then apply constant power control to ILC. This control strategy has a strong applicability for the microgrid network structure, but because of the impact of line parameters, the power calculation is inaccurate. There's no slack node in the system and the power fluctuation will be large. Literature [11] proposes a new virtual coordinate transformation decoupling method for impedance characteristics of low-voltage microgrid. The coordinate rotation angle is the line impedance angle. Good control result can be achieved. Literature [12] adds negative feedback of voltage frequency deviation in the control loop. It improves droop control and reduces the deviation of the target quantity. Till now, the research on the control strategy of hybrid microgrid is still in the early stage.

The operation condition of microgrid can be roughly divided into islanding mode and grid-connected mode. [18][19] In this chapter we explain and verify the control strategy in islanding mode and grid-connected mode separately.

3.1 Islanding mode

Islanding mode is an important operation mode of microgrid. When fault happens in utility grid, the microgrid disconnects from utility grid and turns into islanding mode. Islanding mode can effectively improve system stability and maximize the use of renewable energy. [21] The following discussion is based on the three operating modes: DC sub-network islanding, AC sub-network islanding and AC-DC mixed islanding.

3.1.1 DC sub-network islanding mode

When DC sub-network works in islanding mode, there should be one or more than one DGs provide voltage support for DC sub-network. When master-slave control is applied, a main DG works under voltage control to provide voltage support for the system. Other DGs work under current control to provide power. The master-slave control is strict with the capacity and reliability of the main power supply, and it depends on the communication network. Besides, it is not easy for the system to expand. The master-slave control based on droop control is widely used as a decentralized control method based on local information [49][50]. This section applies a droop control strategy in DC sub-network.

In this model, the DC sub-network consists of a battery, a fuel cell, a photovoltaic cell and DC loads. When DC sub-network works in islanding mode, the battery and the fuel cell work under droop control to provide support for the DC bus voltage. The photovoltaic cell operates in the Maximum Power Tracking (MPPT) mode to make the most use of the renewable energy. The characteristic lines of battery and fuel cell are shown in Figure 3-1.

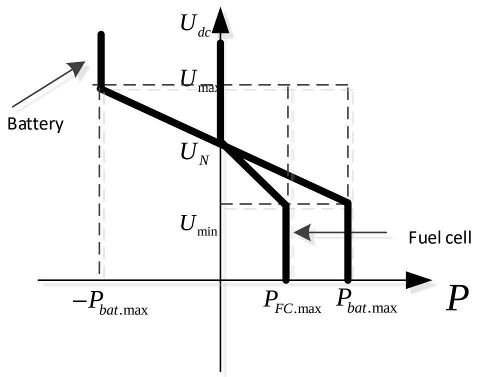

Figure 3- 1 Droop characteristic lines in DC sub-network.

The maximum output power $P_{bat.max}$ of the battery is 75kW. The maximum output power $P_{FC.max}$ of the fuel cell is 50kW. The rated bus voltage U_N is 800V and the maximum voltage error is 5%U_N. The droop coefficient of battery and fuel cell can be calculated by Equation (3-1).

$$k=\frac{U_{max}-U_{min}}{P_{max}-P_{min}} \tag{3-1}$$

The output power of PV at the standard status of 1000W/m^2, 25° C is 50kW. When t=0s, the load is 50kW and the light intensity is 800w/m^2. When t=1s, the load increases 50kW. When t=2s, the load decreases 70kW. When t=3s, the light intensity reduces to 400W/m^2. When t=4s, the light intensity increases to 2000W/m^2. The temperature does not change during the process. Figure 3-2, Figure 3-3 and Figure 3-4 show the output of DGs, load changes and DC bus voltage, respectively.

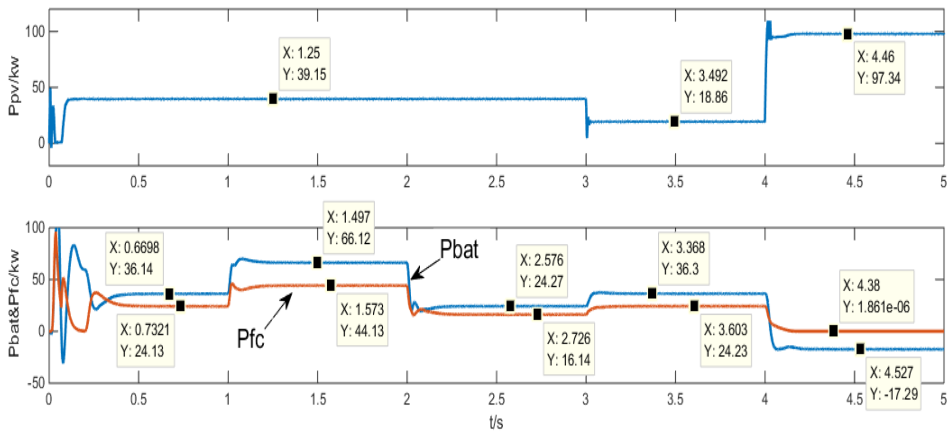

Figure 3- 2 Photovoltaic cell, battery, fuel cell output power.

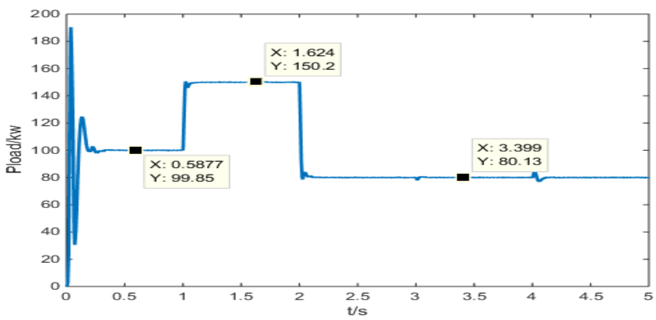

Figure 3- 3 DC load value.

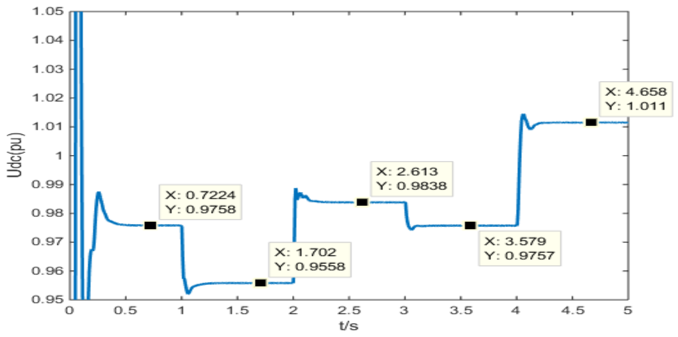

Figure 3- 4 DC bus voltage value.

The data is shown in Table 3-1 (all datum refer to the value in steady state):

Table 3- 1 Datum in DC sub-network islanding mode.

t	Ppv/kW	Pbattery/kW	Pfc/kW	DC load/kW	Udc/pu
0-1s	39.15	36.14	24.13	99.85	0.9758
1-2s	39.15	66.12	44.13	150.20	0.9558
2-3s	9.15	24.27	16.14	80.13	0.9838
3-4s	8.86	36.30	24.23	80.13	0.9757
4-5s	97.34	-17.29	0	80.13	1.011

Neglecting the measurement error and small fluctuations in steady state, the generated power is equal to the total load consumption. The power balance in the DC sub-network can be achieved.

$$P_{pv} + P_{bat} + P_{fc} = P_{load} \tag{3-2}$$

The battery and the fuel cell are able to share the load according to droop coefficient, and the voltage offset corresponds to the preset droop characteristic line.

$$\frac{P_{bat}}{P_{fc}} = \frac{P_{batN}}{P_{fcN}} = \frac{3}{2} \tag{3-3}$$

$$P_{bat} \times k_{bat} = P_{fc} \times k_{fc} = U_N - U \tag{3-4}$$

When t =4-5s, the amount of generated power is greater than the power absorbed by the load. According to the droop characteristic line, the fuel cell is turned off, and the battery alone absorbs the power to maintain the DC bus voltage stability. In DC sub-network islanding mode, through the droop control, the maximum utilization of renewable energy can be achieved and the load is reasonably distributed. The voltage deviation is within the acceptable range.

3.1.2 AC sub-network islanding mode

Similar to the operation of DC sub-network islanding mode, the AC sub-network in this paper also applies droop control in islanding mode. The AC sub-network structure is relatively simple with respect to the DC sub-network. Only the battery provides voltage and frequency support for the AC load.

The scheme of the inverter is shown in Figure 3-5. E is the output voltage of inverter. U is the bus voltage. φ is the phase angle that inverter output voltage phase leads the bus voltage. Z is the line impedance and θ is the impedance angle. P, Q are transmission active and reactive power respectively. Since φ is extremely small, it can be assumed that sinφ≈ φ , cosφ≈1[22].

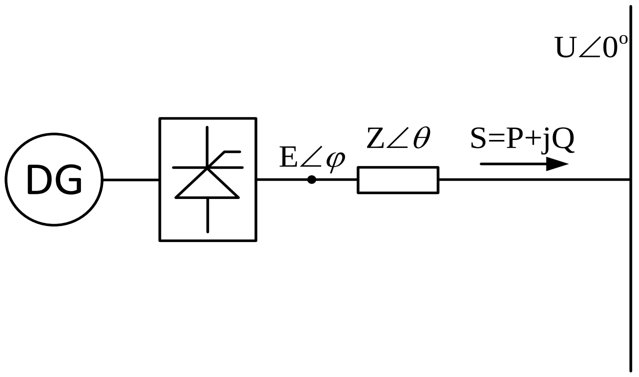

Figure 3- 5 Scheme of the inverter.

The transmission active and reactive power can be calculated by [22]:

$$\begin{cases} P = (\frac{EU}{Z}\cos\varphi - \frac{U^2}{Z})\cos\theta + \frac{EU}{Z}\sin\varphi\sin\theta \\ Q = (\frac{EU}{Z}\cos\varphi - \frac{U^2}{Z})\sin\theta - \frac{EU}{Z}\sin\varphi\cos\theta \end{cases} \tag{3-5}$$

In conventional high voltage transmission lines, the line impendence is mainly inductive(X>>R). θ ≈90°, sin θ ≈1, cos θ ≈0. The transmission power equation can be simplified as:

$$\begin{cases} P = \dfrac{EU}{Z}\varphi \\ Q = \dfrac{U}{Z}(E\text{-}U) \end{cases} \tag{3-6}$$

The active power mainly depends on the phase angle difference φ while the reactive power mainly depends on the voltage difference. The output active power and reactive power can be independently adjusted by the output frequency and voltage of the converter. The droop characteristics are shown as following:

$$\begin{cases} f = f_0 - k_P \times P \\ U = U_0 - k_Q \times Q \end{cases} \tag{3-7}$$

In the formula: f_0, U_0 are the frequency and rated voltage respectively. k_P, k_Q are the active and reactive droop coefficient respectively.

However, in low-voltage microgrid, R >> X. The line impendence is mainly resistive. $\theta \approx 0^o$, sin $\theta \approx 0$, cos $\theta \approx 1$. The transmission power equation can be simplified as:

$$\begin{cases} P = \dfrac{U}{Z}(E\text{-}U) \\ Q = \dfrac{EU}{Z}\varphi \end{cases} \tag{3-8}$$

In this case, the active power mainly depends on the voltage difference, and the reactive power mainly depends on the phase angle difference φ, which is opposite to the high-voltage system. Output active power and reactive power can be independently adjusted through the converter output voltage and frequency. The droop characteristic is shown as:

$$\begin{cases} f = f_0 - k_Q \times Q \\ U = U_0 - k_P \times P \end{cases} \tag{3-9}$$

In the equation: f_0, U_0 are the frequency and rated voltage respectively. k_P, k_Q are the active and reactive droop coefficient respectively.

From the above analysis, it can be seen that in low-voltage microgrids, the characteristics have changed due to its line impedance. As a result, the control strategy is also changed compared with the traditional high-voltage network droop control. In this model, the AC rated voltage is 380V and the DC rated voltage is 800V. The droop control characteristics shown in Equation (3-9) should be applied. The scheme is shown in Fig 3-6.

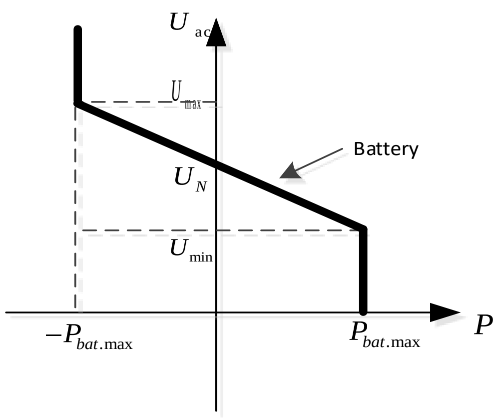

Figure 3- 6 Droop characteristic lines in AC sub-network.

The maximum output power $P_{bat.max}$ of the battery is 150kW. The rated operating point voltage U_N and the frequency f_N are 220V and 50HZ respectively. The maximum voltage deviation is the 5%U_N and the maximum frequency deviation is 0.2HZ. The simulation process of AC sub-network islanding is as following: When t=0s, the load is 50kW. When t=1.5s, the load becomes 150kW, reaching the maximum power output of the battery. When t=3s, the load reduces to 100kW. Load change and voltage frequency waveforms during operation are shown in Figure 3-7 and Figure 3-8.

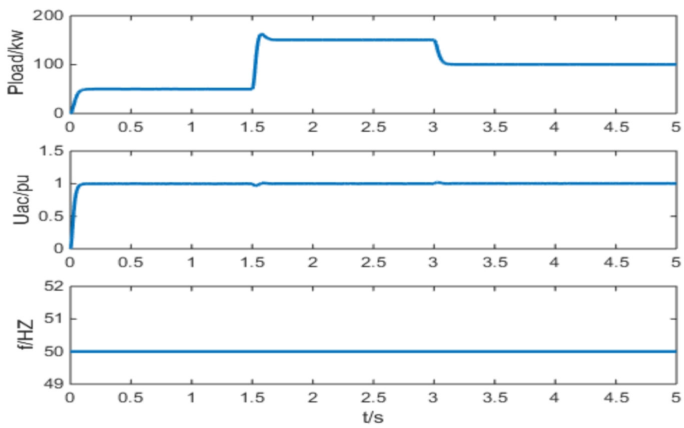

Figure 3- 7 Load and voltage condition in AC sub-network islanding mode.

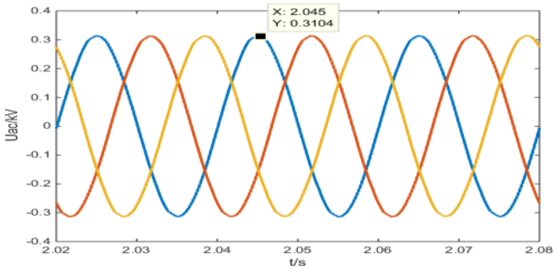

Figure 3- 8 Three-phase AC bus voltage in AC sub-network islanding mode.

During the operation, the voltage and frequency of the AC system can be maintained at the rated value. Only when disturbance occurs, there will be small fluctuation but the magnitude of the disturbance value is within a reasonable range. The three-phase voltage is symmetrical and the voltage peak value is 0.311kV.

3.1.3 AC-DC mixed islanding mode

The mixed islanding operation mode refers to the operation mode in which the PCC switch is disconnected from utility grid and the interlink converter is closed. This is a very important operation mode of hybrid microgrid.

At present, AC-DC mixed island mainly applies the control strategy of AC or DC microgrid. It relies heavily on the structure of hybrid microgrid. In hybrid microgrid which is dominated by DC sub-network, DC bus voltage is supported by DGs in DC sub-network. The voltage and frequency of AC sub-network are controlled through ILC. DGs in AC sub-network work under constant power control. The scheme is shown in Fig 3-9.

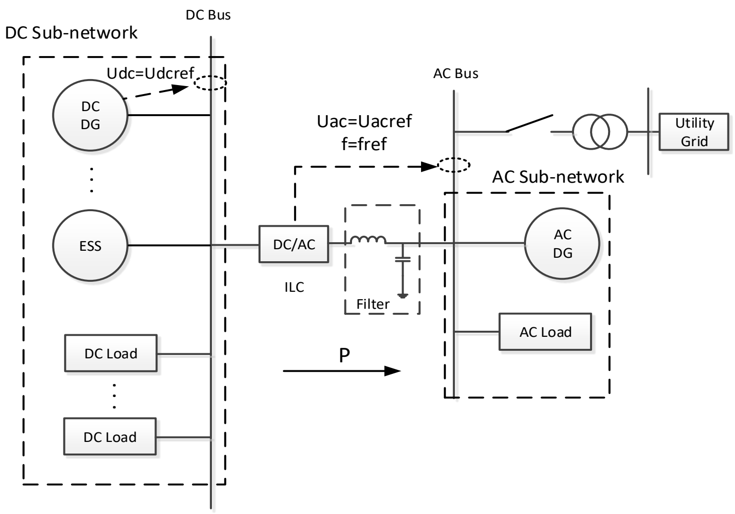

Figure 3- 9 Scheme of hybrid microgrid dominated by DC sub-network.

Similarly, in hybrid microgrid which is dominated by AC sub-network, AC bus voltage and frequency are supported by DGs in AC sub-network. The voltage of DC sub-network is controlled through ILC. DGs in DC sub-network work under constant power control. The scheme is shown in Fig 3-10.

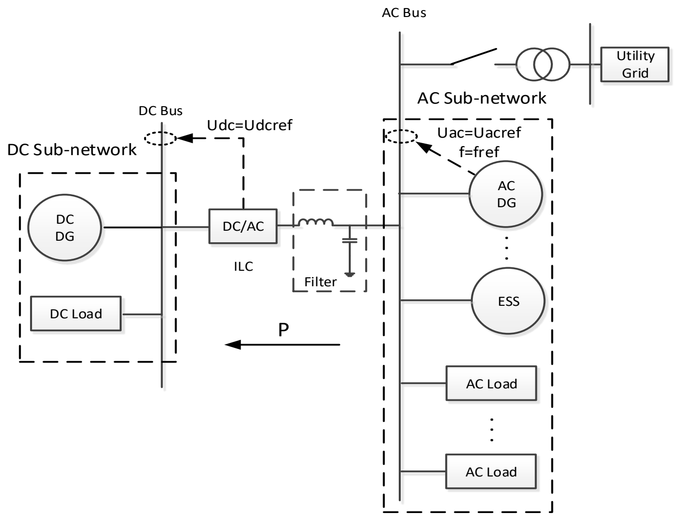

Figure 3- 10 Scheme of hybrid microgrid dominated by AC sub-network.

In the above two control strategies, the energy is transmitted from one side to another. The operation of the whole system depends on the master sources in sub-network, which reduces the reliability and extensibility. Besides, due to the unbalance capacity of AC and DC sub-networks, the capacity of ILC should be very large. What's more, it runs against the concept of local consumption. Large amount of power flows in the system and raises power loss during power transmission.

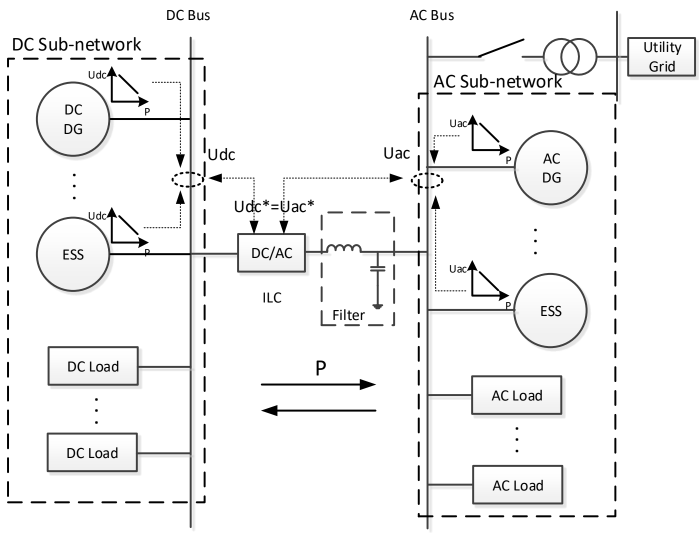

Figure 3- 11 Scheme of entire network droop control.

The research of this paper is based on a small plant in which the AC and DC sub-networks share similar capacity. It is obvious that the above two control strategies are not applicable any more. To solve the drawbacks of the traditional control strategies, the entire network droop control strategy is proposed. The scheme is shown in Fig 3-11.

When fault happens in utility grid, the PCC switch receives the signal and disconnects the microgrid from utility grid, the hybrid microgrid starts to work under mixed islanding mode. DGs in AC sub-network work under P-V, Q-f droop control to provide voltage and frequency reference for the AC system. DGs in DC microgrid work under P-V droop control to provide voltage reference for the DC system. The offset of AC and DC voltage can reflect the load condition in the sub-networks. By measuring and taking the offset of AC and DC bus voltage under control, free power exchange can be achieved between AC and DC sub-network. In this way, the droop control in the entire network can be realized [22].

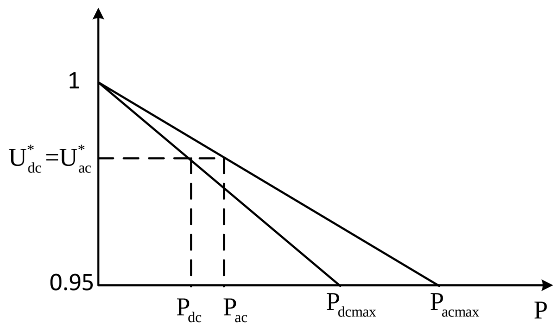

Figure 3- 12 Scheme of entire network droop control.

As shown in Fig 3-12. By unitizing AC and DC bus voltage, the droop characteristic lines of AC and DC sources can be gathered in the same coordinate system. ILC is the bridge between AC and DC sub-network and it plays an important role in the power exchange of two sides. Better load sharing in the entire network can be achieved by controlling AC unit voltage equal to DC unit voltage. Because the voltage value is corresponding to the consumed power, the outer power loop can be modified to voltage loop. The ILC control structure is shown in Fig 3-13.

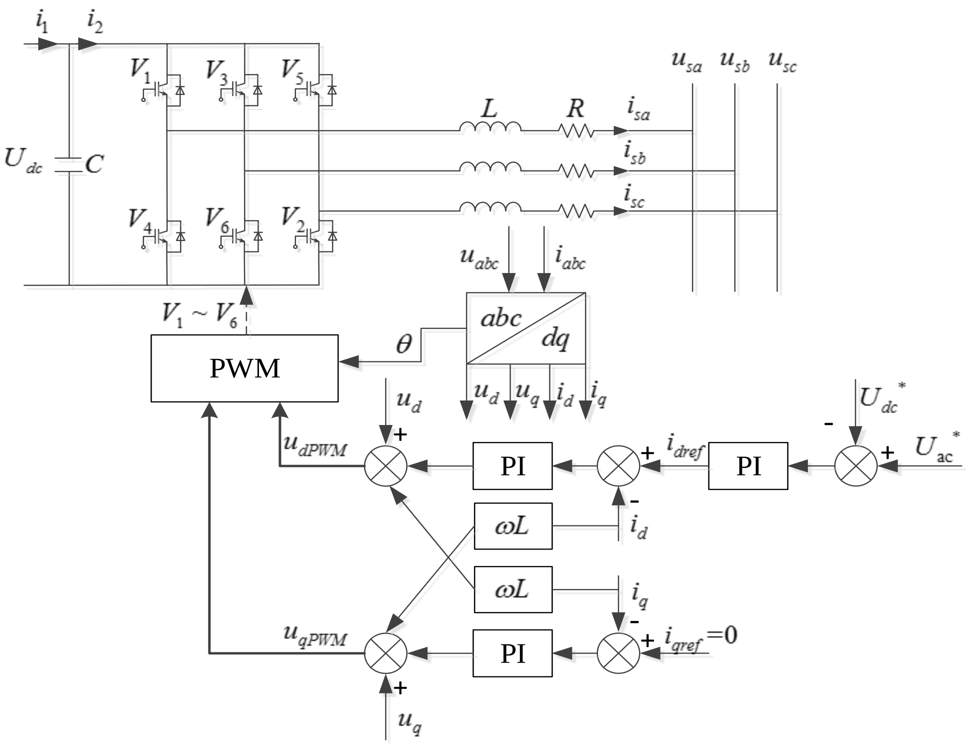

Figure 3- 13 Control structure of ILC.

The control structure still applies active and reactive decoupling control, in which the d-axis outer loop takes AC and DC bus voltage under control and the q-axis outer-loop ensures zero reactive power transmission. The inner current loop responds to the outer loop control target. U_{ac}^* and U_{dc}^* are pu value of AC and DC bus voltage.

When load or output power of PV changes, there will be temporary power unbalance in the microgrid. As a result, voltage drop or rise will occur. By detecting the voltage, ILC can know the load distribution condition in the entire network. When $U_{ac}^*>U_{dc}^*$, it indicates that the DC sub-network supports more load and the voltage offset is greater. The DGs in DC sub-network should reduce output power while DGs in AC sub-network should increase output power. When $U_{ac}^*<U_{dc}^*$, it indicates that the AC sub-network supports more load and the voltage offset is greater. The DGs in AC sub-network should reduce output power while DGs in DC sub-network should increase output power. The modification should keep going until $U_{ac}^*=U_{dc}^*$. The new power balance is achieved. The adjustment process is shown in Fig 3-14.

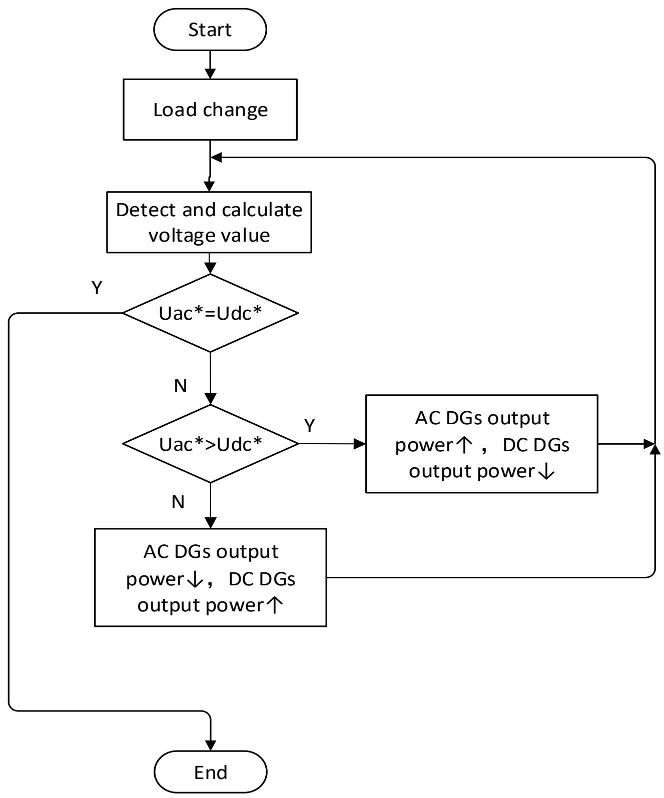

Figure 3- 14 Power adjustment process flow chart.

The entire droop control strategy combines the droop control of AC and DC sub-networks. Better load sharing and maximum use of renewable energy are realized. All DGs make decisions only based on local information, which contributes to higher reliability and extensibility. The control strategy doesn't rely on the structure of hybrid microgrid and can be applied to all kinds of hybrid microgrids.

To verify the control method, assume the simulation process is as follows: Assume the PV panel works at the standard environment of 1000W/m^2, 25^{o}C during the process. The output power of PV is 50kW. When t=0-1s, DC load is 112.5kW and AC load is 75kW. When t=1-2s, DC load is 112.5kW and AC load is 150kW. When t=2-3s, DC load is 175kW and AC load is 150kW. When t=3-5s, DC load is 175kW and AC load is 75kW. The PV output and load change are summarized in Table 3-2.

Table 3- 2 Load and P_{pv} change in mixed islanding mode.

t/s	DC Load/kW	AC Load/kW	P_{pv}/kW
0-1	112.5	75	50
1-2	112.5	150	50
2-3	175	150	50
3-5	175	75	50

The value of AC&DC load, AC&DC bus voltage and exchanged power of ILC are shown in Figure 3-15, Figure 3-16.

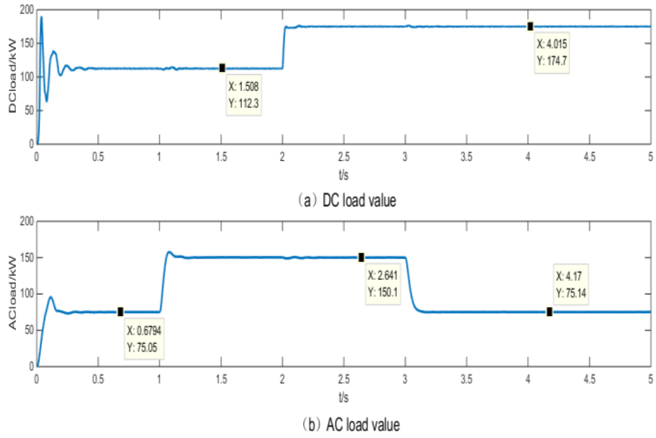

Figure 3- 15 Load change in mixed islanding mode.

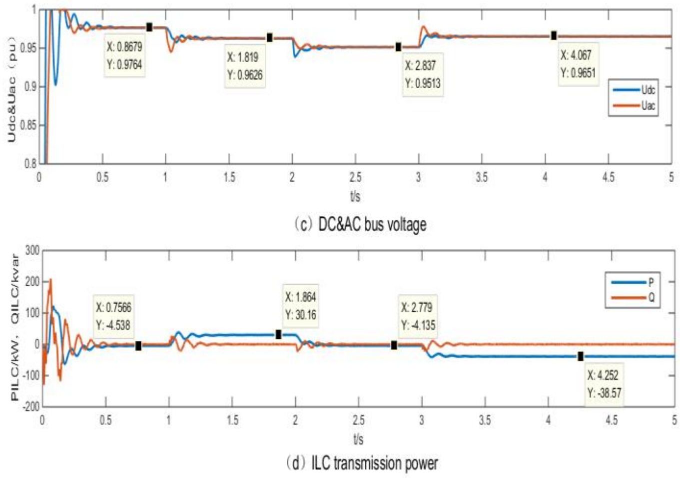

Figure 3- 16 Bus voltage and ILC transmission power in mixed islanding mode.

With the change of load, the unit value of AC and the DC voltage can be consistent under the proposed control strategy. The load can be evenly shared in the entire network. ILC provides the required active power transmission between AC and DC sub-network (assume that from DC sub-network to AC sub-network is positive direction). The reactive power transmission is controlled to be 0.

In the following, the comparison between actual value and calculated value of voltage is made to verify the proposed control strategy. P_{ILC} is the active power transmitted by ILC, which is positive from DC sub-network to AC sub-network. The actual output power of DGs in DC sub-network is P_{DC}:

$$P_{DC} = DCload - P_{pv} + P_{ILC} \tag{3-10}$$

The actual output power of DGs in AC sub-network is P_{AC}:

$$P_{AC} = ACload - P_{ILC} \tag{3-11}$$

The simulated value of AC and DC bus voltage is Uac and Udc respectively. The calculated value of AC and DC bus voltage is Udc* and Uac* respectively:

$$U_{dc}^{*} = 1 - 0.05 \times \frac{P_{DC}}{125} \tag{3-12}$$

$$U_{ac}^{*} = 1 - 0.05 \times \frac{P_{AC}}{150} \tag{3-13}$$

The AC and DC bus voltage errors can be calculated by:

$$\Delta U_{dc}\% = \frac{|U_{dc} - U_{dc}^{*}|}{U_{dc}} \times 100\% \tag{3-14}$$

$$\Delta U_{ac}\% = \frac{|U_{ac} - U_{ac}^{*}|}{U_{ac}} \times 100\% \tag{3-15}$$

The datum of mixed islanding mode is shown in Table 3-3.

Table 3- 3 Datum in AC-DC mixed islanding mode.

t/s	0-1	1-2	2-3	3-5
PILC/kW	-4.538	30.16	-4.135	-38.57
PDC/kW	57.962	92.66	120.865	86.43
PAC/kW	79.538	119.84	154.135	113.57
Udc(Uac)	0.9765	0.9627	0.9513	0.9651
Udc*	0.9768	0.9629	0.9517	0.9654
Uac*	0.9734	0.96	0.9486	0.9621
ΔUdc%	0.03%	0.02%	0.04%	0.03%
ΔUac%	0.35%	0.28%	0.28%	0.31%

As can be seen from Table 3-3, the errors between the calculated value and the measured value of AC and DC bus are less than 1%, which is mainly caused by the measurement error and the line impedance. The errors are within the allowable range. The AC-DC mixed islanding control strategy based on entire network droop control works.

3.2 Grid-connected mode

The grid-connected operation mode is another important operation mode of microgrid and it is the most common operating mode of microgrid. In grid-connected mode, microgrid is connected to utility grid and the PCC switch is closed to enable power exchange between microgrid and utility grid. In this mode, utility grid provides voltage and frequency support for AC sub-network. Renewable sources in AC sub-network work in MPPT control to generate maximum power. Energy storage system absorbs the power to charge, then shuts off when the energy is sufficient. DC sub-network is connected to AC bus through ILC and operates as an active load of AC sub-network. Renewable sources in DC sub-network also works in MPPT mode and energy storage system absorbs power or shuts off. In grid-connected operation, AC sub-network, DC sub-network, and utility grid can realize free flow of power in the network through ILC and PCC switches to balance power fluctuations caused by output changes and load changes.

In this model, when microgrid works in grid-connected mode, PV works in MPPT control. The reference power of fuel cell and batteries are 0. DC bus voltage is controlled by AC sub-network through ILC. AC bus voltage and frequency are provided by utility grid. In order to verify the proposed control strategy of AC/DC hybrid microgrid, the following simulation is performed. When t=0s, light intensity is 400 W/m^2. PV works in maximum power tracking state and the output power is 20kW. DC and AC loads are 30kW and 10kW, respectively. When t=1s, AC load increases 20kW. When t=3s, DC load increases 20kW. Light intensity becomes 1000W/m^2 and PV output power becomes 50kW. When t=4s, DC load reduces 40kW. PV output power and load change are summarized in Table 3-4.

Table 3- 4 Load and P_{pv} change in grid-connected mode.

t/s	DC Load/kW	AC Load/kW	Ppv/kW
0-1	30	10	20
1-2	30	30	20
2-3	50	30	20
3-4	50	30	50
4-5	10	30	50

AC and DC load, PV output power are shown in Figure 3-17.

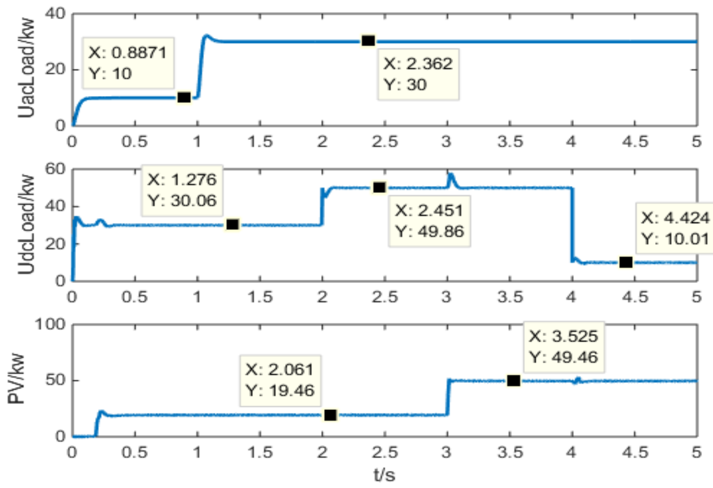

Figure 3- 17 AC&DC load, photovoltaic cell output power in grid-connected mode.

Power balance is achieved in DC sub-network through the control of ILC:

$$P_{pv} - DCload = P_{ILC} \tag{3-16}$$

Power balance is achieved in AC sub-network through PCC by utility grid:

$$P_{ILC} - ACload = P_{grid} \tag{3-17}$$

In Equation (3-17): ACload is the value of AC load; P_{grid} is the exchanged power with utility grid (from microgrid to utility grid is positive).

For the entire microgrid, the power balance equation is:

$$P_{pv} - DCload - ACload = P_{grid} \tag{3-18}$$

Equation(3-18) is a combination of Equation(3-16) and Equation(3-17).

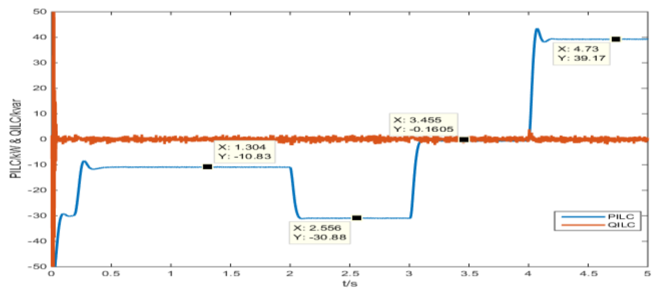

Figure 3- 18 ILC transmission power in grid-connected mode.

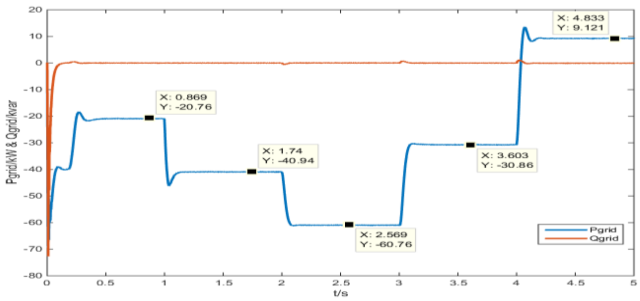

Figure 3- 19 PCC transmission power in grid-connected mode.

As shown in Figure 3-18 and Figure 3-19, when t=1-3s, load of DC sub-network is large. PV output power is insufficient to maintain power balance in DC sub-network. ILC absorbs power from AC subnetwork. When t=3-4s, PV output power is equal to the value of DC load. DC sub-network can maintain its own power balance and ILC transmission power equals to 0. When t=4-5s, DC load is small. PV generates excess power and the excess power is transferred to AC sub-network through ILC. As shown in the figures, when t=1-4s, generated power is smaller than consumed power in microgrid. Microgrid absorbs power from utility grid. When t=4-5s, generated power is greater than consumed power in microgrid. Microgrid transfers excess power to utility grid.

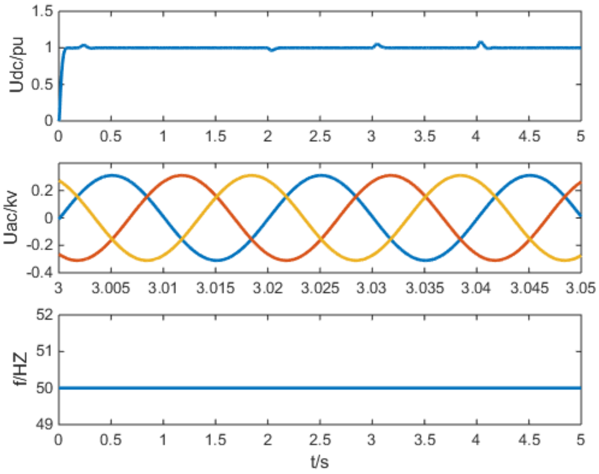

Figure 3- 20 Bus voltage and frequency in grid-connected mode.

In grid-connected mode, DC bus voltage is controlled by AC sub-network through ILC. With the change of load and generated power of DGs, there will be small fluctuations within a reasonable range, but it can be quickly suppresssed to the rated value. AC bus voltage frequency is provided by utility grid and can be kept constant as shown in Figure 3-20.

3.3 Summary

This chapter mainly discussed about the control strategies of islanding and grid-connected operation modes of hybrid microgrids based on a small plant. Islanding operation is divided into three operating modes: DC sub-network islanding mode, AC sub-network islanding mode and AC-DC mixed islanding mode. An entire network droop control strategy of mixed islanding mode is proposed. It can realize a better load sharing in the whole network and increase the stability of the system. During grid-connected operation, the large power grid provides voltage and frequency support for the AC sub-network. ILC provides voltage support for the DC sub-network to ensure stable operation of the system. Simulation results based on PSCAD show that the control strategies proposed in this chapter can achieve good control effect both in grid-connected and islanding modes.

4 A SMOOTH TRANSITION METHOD BASED ON ISLANDING SIGNAL

4.1 The origin of transient impact

As mentioned before, microgrid has two operation modes: grid-connected mode and islanding mode. In most cases, microgrid operates in grid-connected mode. When external fault happens or power quality cannot meet the requirements, microgrid disconnects from utility grid by PCC switch and enters islanding mode to provide continuous power supply for local load to ensure reliability of power supply. When external fault is cleared, PCC switch is closed again and microgrid connects to utility grid again. In the transition process of two modes, large impacts occur. The issue of smooth transition of microgrid is another important issue of microgrid.

Literature [53] focuses on a smooth transition control method based on regulator state follower when switching from grid-connected mode to islanding mode. In Literature [54], an adaptive droop coefficient method is proposed to reduce voltage deviation, thereby reducing the transition impact. Literature [55] studies the timing coordination of mode switching and physical switching in the process of micro-grid operating state switching.

In the control strategy proposed in this paper, the microgrid operates in islanding mode, the battery and fuel cell in DC sub-network apply voltage control. The battery in AC sub-network applies VF control. When microgrid operates in grid-connected mode, all DGs operate in power control. In order to implement different control strategies for islanding mode and grid-connected mode, each DG needs two sets of controllers: voltage controller and power controller. Both voltage controller and t power control adopt the control structure of double loop PI control. The control structure of PI regulator is shown in Figure 4-1.

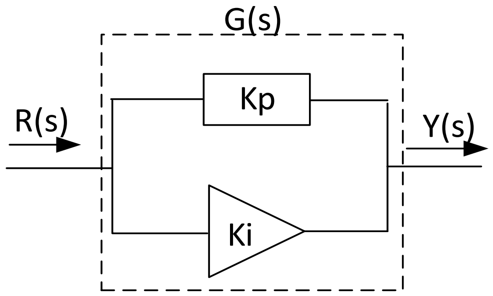

Figure 4- 1 PI regulator structure.

K_p is the integral gain and K_i is the proportional gain.

The PI regulator transfer function is:

$$G(s) = K_p + \frac{K_i}{s} \tag{4-1}$$

When microgrid operates in islanding mode, the voltage controller is put into operation. The power controller is also working during this time, but the output control signal does not act on the converter. Similarly, when microgrid operates in grid-connected mode, the power controller is put into operation. The voltage controller is working at the same time, but the output control signal does not act on the converter. When the two modes are switched, because of the memory of PI regulator integral part, there will be a step change of regulator output value, which causes a sudden change in the current reference value and leads to an impact on the electrical quantity. In some serious situation, it can even cause oscillation.

In addition to the impact caused by the output state of the regulator, when the microgrid is switched from islanding mode to grid-connected mode, there will be voltage amplitude, phase, and frequency differences between microgrid and utility grid. It will cause great rush current at PCC as well.

4.2 Transient impact suppression methods

4.2.1 Suppression method based on regulator state follower

From the above section, we can see that in order to apply different control modes in different operating modes, the switching of different controllers needs to be completed at the moment of switching. The traditional controller adopts the structure of double PI regulator loop. Due to the existence of the integral part, the regulator output has a memory function. The sudden change of the regulator output at the instant of switching is the reason of the impact during the transition of different operation modes. [52]

In order to solve the problem of abrupt change of regulator state, a method based on regulator state follower has been proposed. When microgrid is switched from grid-connected mode to islanding mode, DGs are switched from power control to power control. The output of the power control regulator should be applied as the input reference of the voltage control regulator. The output of both sets of regulators always remain in the same state [52]. The scheme of regulator state follower is shown in Figure 4-2.

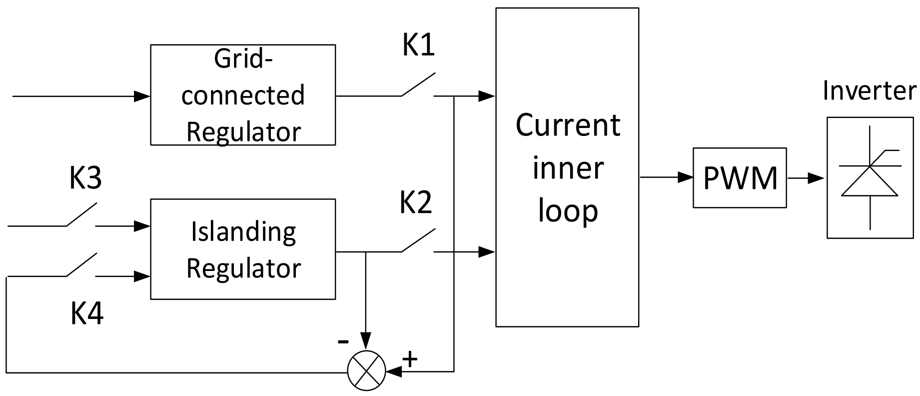

Figure 4- 2 Scheme of regulator state follower from grid-connected mode to islanding mode.

During grid-connected period, K1&K4 are closed and K2&K3 are opened. At this time, power controller works to control DG’s output power. Voltage controller follows the output state of power controller. When it is detected that the microgrid disconnects from utility grid, K2&K3 are closed and K1&K4 are opened. The control mode is switched and microgrid turns into islanding mode. Because the state follower maintains the output value of voltage control regulator equal to the output of power control regulator, there is no abrupt change in the reference value of the inner current loop at the instant of switching, which reduces the transient impact of electric quantity.

When microgrid is switched from islanding mode to grid-connected mode, DGs need to switch from voltage control to power control. The output of voltage control regulator is applied as the input reference of the power control regulator. The regulator state is synchronized followed [53]. The scheme of state follower is shown in Figure 4-3:

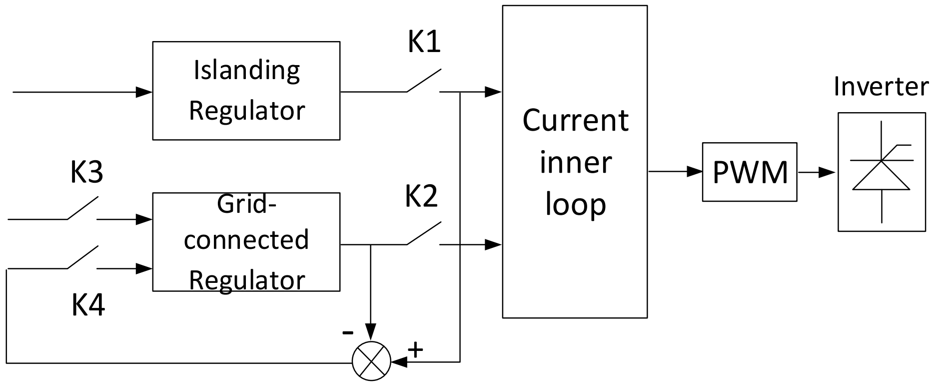

Figure 4- 3 Scheme of regulator state follower from islanding mode to grid-connected mode.

The theory of above two state followers is similar. During islanding period, K1&K4 are closed and K2&K3 are opened. At this time, voltage controller works to control the voltage and frequency of AC sub-network and the voltage of DC sub-network. Power controller follows the output state of voltage controller. When it is detected that the PCC switch is closed, K2&K3 are closed and K1&K4 are opened. The control mode is switched and microgrid works in grid-connected mode. Because the state follower always keeps the output value of the power control regulator equal to the output of voltage control regulator, there is no abrupt change in the reference value of the inner current loop at the moment of switching, which reduces the transient impact of electric quantity.

In addition to the sudden change of the regulator state, voltage and frequency difference between microgrid and utility grid can also cause transient impact in the switch from islanding mode to grid-connected mode. In order to solve this problem, it is necessary to perform pre-synchronization operation before the switch operation [54]. The pre-synchronization control scheme is shown in Figure 4-4.

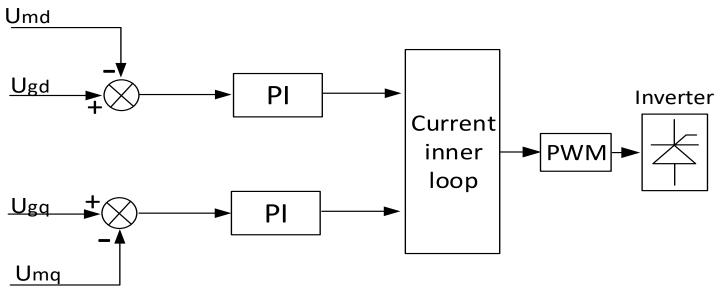

Figure 4- 4 Pre-synchronization control scheme.

U_{gd} and U_{gq} in the figure refer to the dq0 coordinates voltage of utility grid. U_{md} and U_{mq} refer to the dq0 coordinates voltage of the micro grid. Through Parker transformation, the three-phase AC voltage is transformed into DC voltage in the dq0 coordinate, which avoids the direct adjustment of voltage and frequency. What's more, it realizes the linear control of the voltage. When islanding signal is detected, the pre-synchronization control is put into operation. When the voltage and frequency deviation of both sides are with the acceptable range, PCC closes and pre-synchronization control stops working. Micro-grid switches to grid-connected mode successfully.

4.2.2 Suppression method based on islanding signal

The traditional smooth transition method suppresses transient impact by applying state follower to keep the state value of two controllers equal. The state follower can theoretically realize the synchronization of the output states of the controllers. However, there are some defects of the traditional method based on state follower. In the smooth transition method based on state follower, PI regulator not only needs to complete the outer loop control target, but also realizes the state following. As a result, the parameters of PI regulator are difficult to set and the control effect is not good. What's more, when the operating state is frequently switched in a short period, the regulator has no time to respond. The regulator state will change abruptly, which has a bad effect on smooth transition.

In order to solve the above problems, this paper proposes a novel smooth transition method based on islanding signal. The control scheme is shown in Figure 4-5.

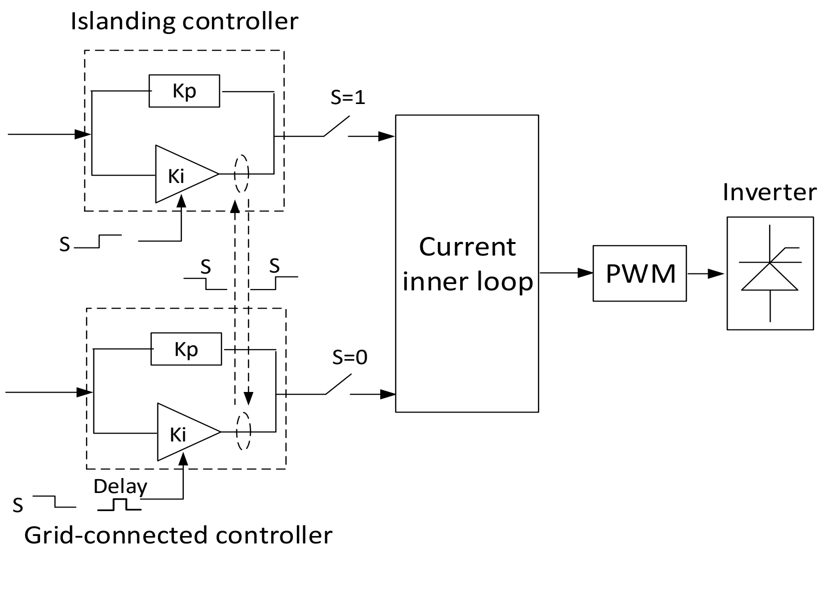

Figure 4- 5 Scheme of islanding signal method.

The entire control structure consists of outer loop and inner loop. The output signal of current inner loop is used to generate the control signal of inverter. S is islanding signal. When microgrid works in grid-connected mode, S=0 and power control regulator works. When microgrid works in islanding mode, S becomes 1 and voltage control regulator works. Figure 4-5 shows the outer loop of the controller. K_p is proportional part and can respond to the input signal instantly. K_i is integral part. The static error is eliminated by integrating the input error. The memory of the integral part state is the main reason of the transient impact.

When microgrid switches from grid-connected mode to islanding mode, the islanding signal S generates a falling edge from 1 to 0. The falling edge triggers the power control outer loop regulator to renew its state value. The renewed value is the detected state value of voltage control outer loop regulator at this time. When microgrid switches from islanding mode to grid-connected mode, the islanding signal S generates a rising edge from 0 to 1. The rising edge triggers the voltage control outer loop regulator to renew its state value. The renewed value is the detected state value of power control outer loop regulator at this time. What's different is that the rising edge of islanding signal should work on the power control regulator after a delay. During the delay period, the pre-synchronization control is performed.

In this way, the output states of two sets of controllers are sure to be the same at transient instant. The problem of the transition impact can be solved from the root and it can be applied in all cases. At the same time, since the outer loop is only applied to achieve the control target, the set of regulator parameter is greatly simplified.

4.3 Simulation

4.3.1 Comparison of different transition methods

In order to verify the new smooth transition method proposed in this thesis, simulation is carried out in this section. The simulation includes direct transition method, traditional smooth transition method based on regulator state follower and proposed new smooth transition method based on islanding signal. Through the simulation results, the advantages and disadvantages of each switching mode are compared and analysed. During the simulation process, the circuit parameters and control parameters are kept the same.

The simulation process is as follows: when t=0-1.5s, microgrid operates in grid-connected mode. When t=1.5s, microgrid turns to islanding mode. PCC switch is disconnected and the control mode is changed. When t=3s, microgrid turns to grid-connected mode again. After pre-synchronization operation, PCC switch is closed and the control mode is switched back to grid-connected mode. During the process, the PV output power, DC load and AC load are 50 kW, 112.5 kW and 75 kW respectively.

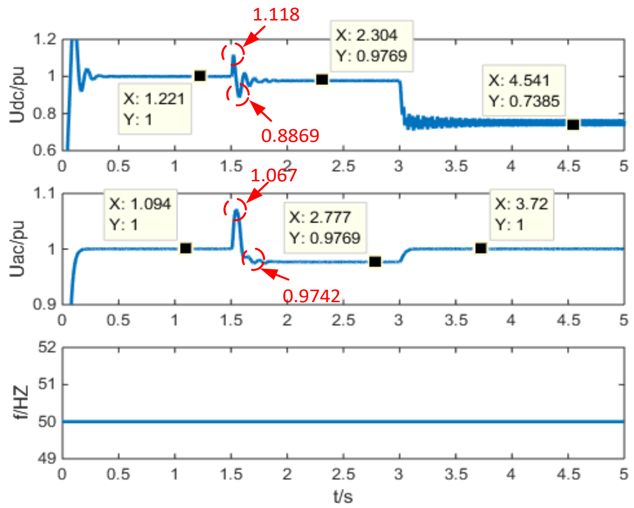

Figure 4- 6 DC voltage, AC voltage and frequency of direct transition method.

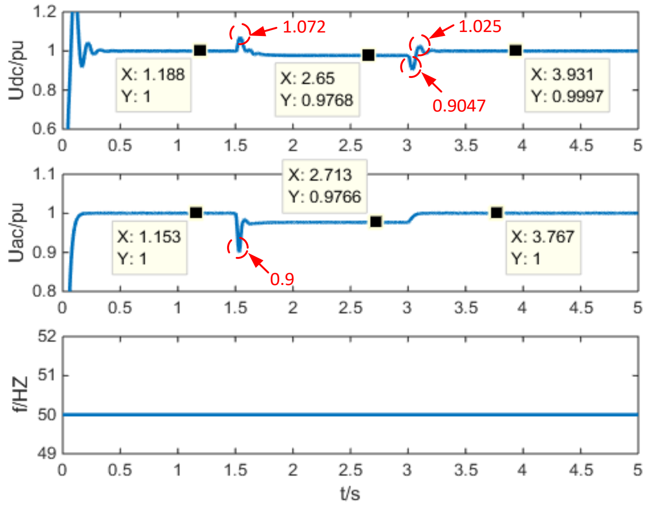

Figure 4- 7 DC voltage, AC voltage and frequency of traditional smooth transition method.

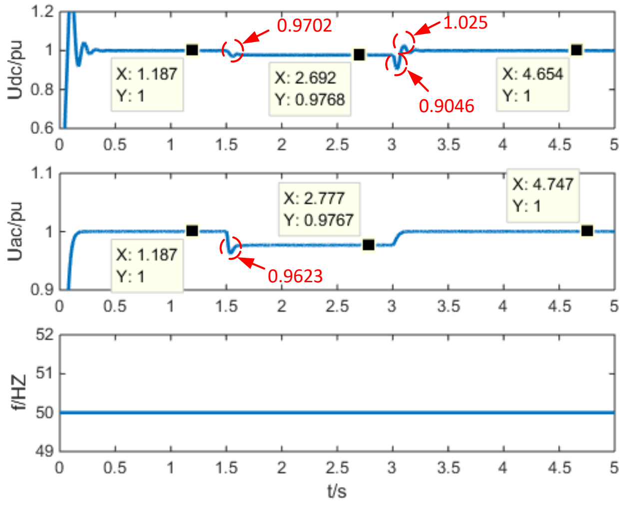

Figure 4- 8 DC voltage, AC voltage and frequency of proposed smooth transition method.

The DC bus voltage, AC bus voltage and frequency reflect the stability of the hybrid microgrid. The DC voltage AC voltage and frequency waveforms corresponding to direct transition method, traditional transition method based on state follower and novel transition method based on islanding signal proposed in this thesis are shown in Figure 4-6, Figure 4-7, and Figure 4-8, respectively. The datum during the process is shown in Table 4-1 and Table 4-2.

Table 4- 1 Hybrid microgrid operating status from grid-connected mode to islanding mode.

Transition method	ΔU_{dcmax}	ΔU_{acmax}	Transition time	Succeed? (Y/N)
Direct transition	11.31%	6.7%	0.46s	Y
Traditional smooth transition	7.2%	10%	0.31s	Y
Novel smooth transition	2.98%	3.77%	0.25s	Y

Table 4-1 shows the datum of voltage offsets, switching duration and switching result of each transition method from grid-connected mode to islanding mode. All three methods can complete the transition from grid-connected mode to islanding mode successfully, but the DC voltage offset, AC voltage offset and switching time of novel switching method are the smallest among all the methods. The effect of novel smooth transition method is the best. Among them, the DC voltage offset and the switching time of direct switching method are the largest. The AC voltage offset of traditional smooth transition method is the largest.

Table 4- 2 Hybrid microgrid operating status from islanding mode to grid-connected mode.

Transition method	Δ U_{dcmax}	Δ U_{acmax}	Transition time	Succeed? (Y/N)
Direct transition	26.15%	2.31%	—	N
Traditional smooth transition	9.53%	2.34%	0.23s	Y
Novel smooth transition	9.54%	2.33%	0.23s	Y

Table 4-1 shows the datum of voltage offsets, switching duration and switching result of each transition method from islanding mode to grid-connected mode. The direct transition method fails to complete the transition of mode and the DC voltage offset is very large. The traditional smooth switching mode and the new smooth switching mode are basically the same in voltage offset and transition time. The datum are all within an acceptable range.

In order to analyse the simulation results shown in Table 4-1 and Table 4-2, the PI regulator state in each transition method is observed. Figure 4-9, Figure 4-10, and Figure 4-11 show the regulator output state of DGs and ILC in direct transition method, traditional smooth transition method, and novel smooth transition method, respectively.

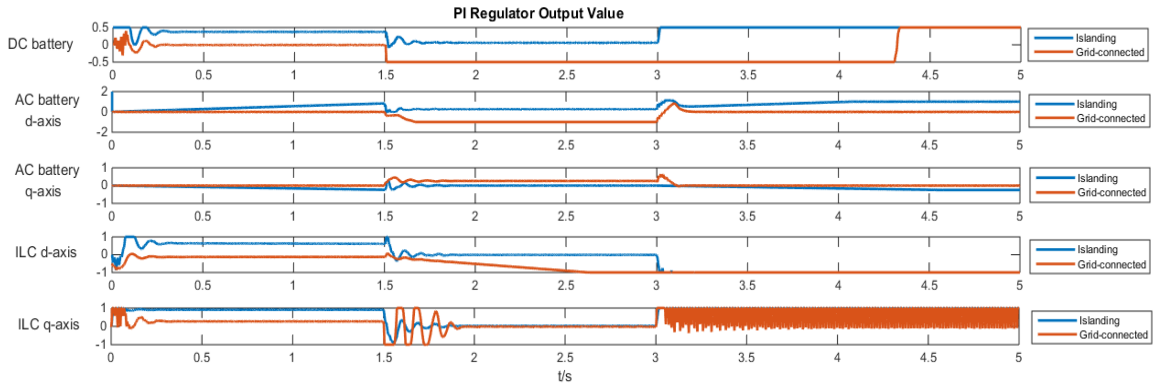

Figure 4- 9 Regulator state of direct transition method.

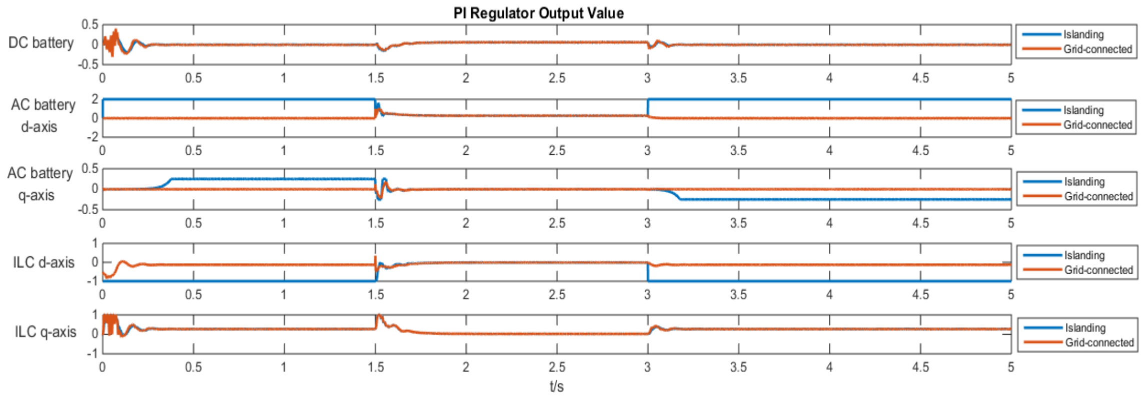

Figure 4- 10 Regulator state of traditional smooth transition method.

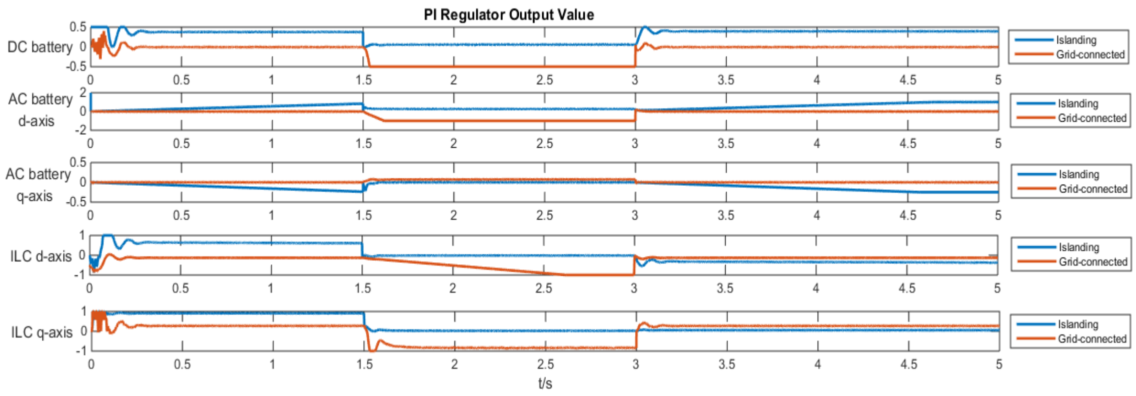

Figure 4- 11 Regulator state of novel smooth transition method.

When t=0-1.5s, microgrid operates in grid-connected mode. Since the direct transition method does not realize the regulator state following, there is a large step change of state at the transition instant. As a result, the DC voltage has a large mutation and the switching time is long. In traditional smooth transition method, a state control follower is used to keep the output states of the two controllers consistent. When grid-connected controller is working, the islanding controller will follow the output state of grid-connected controller, as shown in Figure 4-10. The q-axis current of DC battery and ILC can realize the state following successfully. Therefore, the DC voltage offset in the traditional smooth transition method is smaller than direct transition method. However, because the control parameters of the islanding controller are set for islanding operation mode, the regulators of AC battery and ILC d-axis all reach a saturation state and cannot realize state following successfully. The step change of regulator state in the switching time even larger than that in direct transition method. Therefore, in traditional smooth transition method, the AC voltage offset is the largest. When t=1.5-3s, microgrid operates in islanding mode. When operating mode is switched at t=3s, direct transition method fails because the step change in regulator is too large. The traditional smooth transition method achieves a good state following effect and realizes smooth transition, as shown in Figure 4-10.

The novel smooth transition method can ensure no step change of regulator state at any transition moment to realize smooth transition between grid-connected mode and islanding mode. During the transition from grid-connected mode to islanding mode at 1.5s, the effect of novel smooth transition method is better than both of the other two transition methods. During the transition from islanding mode to grid-connected mode at 3s, the effect is similar to that of traditional smooth transition method because it realizes regulator state following during 1.5s to 3s.

4.3.2 Influence of load change on smooth transition

The AC/DC hybrid microgrid is more complex than the traditional microgrid, and the energy can flow freely through ILC in AC and DC sub-networks. Based on the novel smooth transition method proposed in the previous section, this section discussed about the impact of load value on smooth transition.

The simulation process is as follows: when t=0s, microgrid starts in grid-connected mode. When t=1.5s, PCC switch opens and microgrid turns to islanding mode. When t=3s, PCC switch closes and microgrid turns to grid-connected mode again. During the process, PV output power is 50kW. DC load is s 112.5kW. AC load is 30kW, 75kW, 120kW and 150kW respectively. The waveforms of DC voltage, AC voltage and ILC transmission power are shown in Figure 4-12, Figure 4-13, Figure 4-14, and Figure 4-15, respectively.

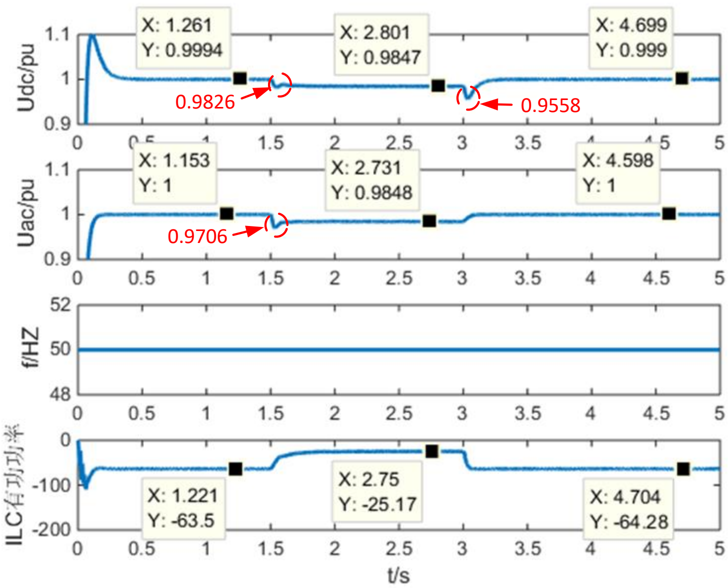

Figure 4- 12 DC voltage, AC voltage, frequency and ILC transmission power.

（DC load=112.5kW, AC load=30kW）

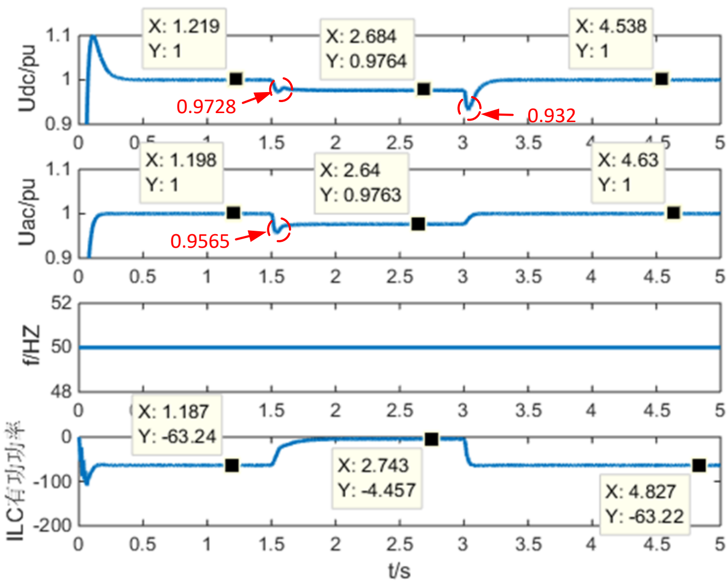

Figure 4- 13 DC voltage, AC voltage, frequency and ILC transmission power.

（DC load=112.5kW, AC load=75kW）

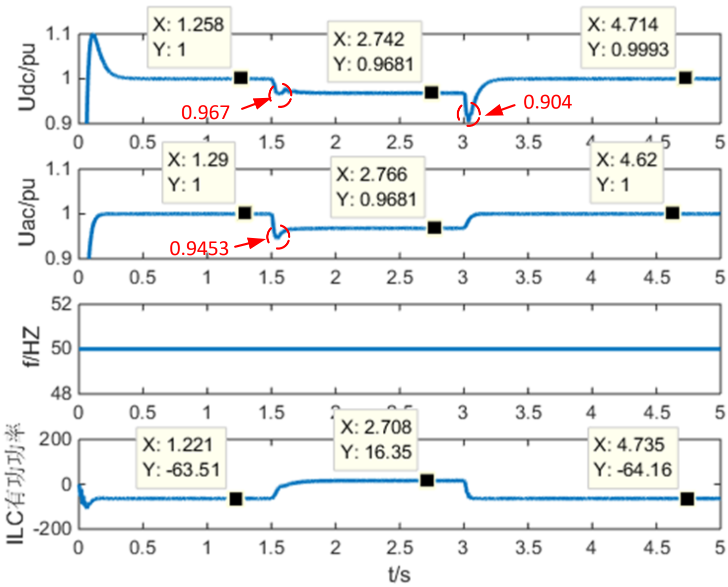

Figure 4- 14 DC voltage, AC voltage, frequency and ILC transmission power.

（DC load=112.5kW, AC load=120kW）

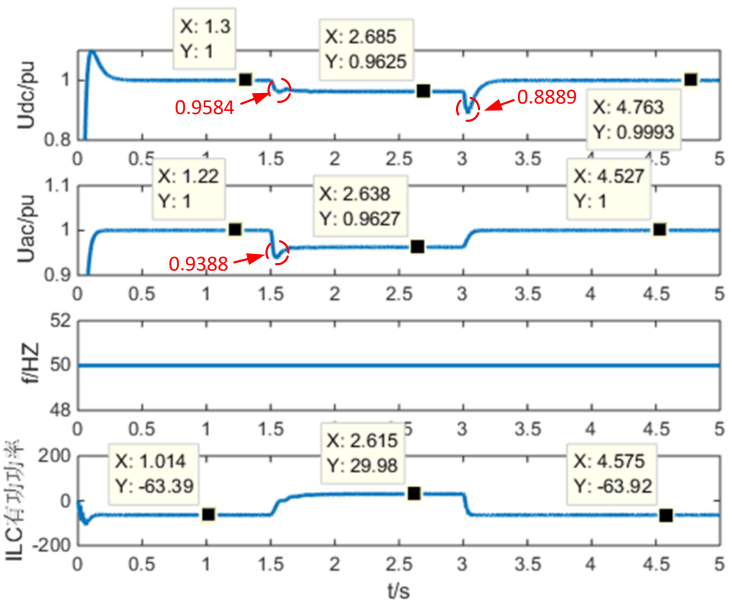

Figure 4- 15 DC voltage, AC voltage, frequency and ILC transmission power.

（DC load=112.5kW, AC load=150kW）

The datum of simulation is shown in Table 4-3, including DC load value *DCLoad*, AC load *ACLoad*, photovoltaic cell output power P_{pv}, ILC transmission power P_{ILC1} in grid-connected mode, ILC transmission power P_{ILC2} in islanding mode, ILC transmission power ΔILC at the instant of mode transition, DC voltage maximum change ΔU_{dc1} from grid-connected mode to islanding mode, DC voltage maximum change ΔU_{dc2} from islanding mode to grid-connected mode and AC voltage maximum change ΔU_{ac}.

Table 4- 3 AC/DC hybrid microgrid operating state.

DCLoad/kW	ACLoad/kW	Ppv/kW	PILC1/kW	PILC2/kW	ΔILC/kW	ΔUdc1	ΔUdc2	ΔUac
112.5	30	50	-63.5	-25.17	38.33	0.24%	2.96%	1.4%
112.5	75	50	-63.5	-4.46	59.04	0.35%	4.53%	2.04%
112.5	120	50	-63.5	16.35	79.85	0.42%	6.61%	2.37%
112.5	150	50	-63.5	29.98	93.48	0.47%	7.69%	2.48%

As can be seen from the datum in Table 4-3, since PV output power and DC load do not change during the process, P_{ILC1} does not change during grid-connected operation and equals to the power absorbed by DC sub-network. With the increase of AC load, the transmission power of ILC increases during islanding operation. As a result, the power change during transition instant increases, resulting in an increase in voltage offset during transition process, as shown in Figure 4-16. In summary, load value will affect smooth transition of hybrid microgrid. The greater the unbalanced power in AC/DC sub-network, the more unfavourable smooth transition is.

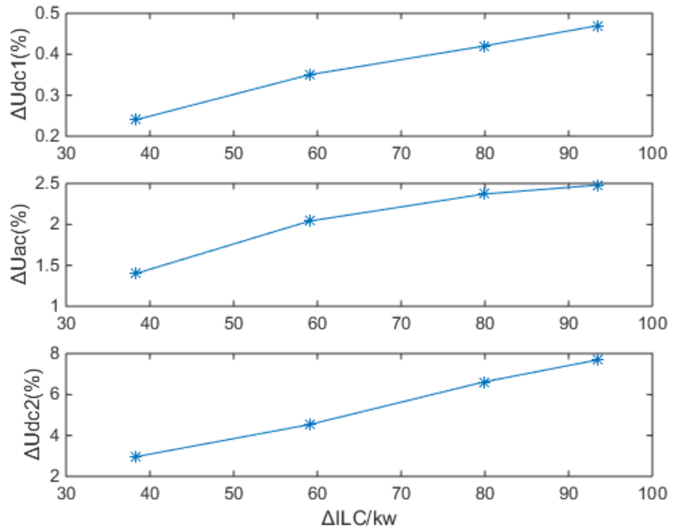

Figure 4- 16 Maximum variation of AC and DC voltage.

Droop control strategy is applied in this thesis and the change of load corresponds to the drop of voltage. The heavier the load, the bigger the voltage drop is, which correspond to bigger voltage change during transition. This is the reason why load change can influence smooth transition. To solve this problem, a secondary regulator can be added to compensate the drop of voltage, which will be discussed in the future.

4.4 Summary

This chapter first introduces the cause of shock during mode transition, which provides the theoretical basis for smooth transition methods. Then, the traditional regulator state follower is summarized and a novel smooth transition method based on based on islanding signal is proposed. Finally, the simulation proves the superiority of the novel smooth transition method. Based on the proposed method, the influence of the load on hybrid microgrid smooth transition is also studied. Simulation results show that the greater the unbalanced power in AC/DC sub-network at transition instant, the greater the impact on the smooth transition.

5 CONCLUSION

5.1 Conclusion

Hybrid microgrid is suitable for the access of various AC/DC distributed generators and loads. It can reduce the use of redundant convertors and improve the efficiency of power consumption. It is the future of the microgrid. This thesis focuses on the control strategy of AC/DC hybrid microgrid. It builds a hybrid microgrid model based on a small plant. A control strategy which is suitable for hybrid microgrids with similar AC and DC sub-network capacity is proposed. Simulation of the operation modes such as DC sub-network islanding, AC sub-network islanding, mixed islanding and grid-connected modes are carried out. Based on the proposed control strategy, the smooth transition problem between mixed islanding mode and grid-connected mode is studied. A novel smooth transition method of AC/DC hybrid microgrid is proposed and verified by simulation. The conclusions of this thesis are as follows:

1) A model of hybrid microgrid with PV cell, fuel cell, batteries and AC/DC loads in a small plant is built. Based on the PSCAD/EMTDC simulation software, the DGs and their interface converters are discussed. The simulation verifies the validity of different control strategies of DGs.

2) A control strategy for hybrid microgrid with similar capacity of AC and DC sub-network is proposed. In grid-connected mode, utility grid provides voltage and frequency support for AC sub-network. AC sub-network provides the voltage support for DC sub-network through ILC. In islanding mode, the entire network droop control strategy is applied. AC and DC sub-networks share AC and DC loads together through power exchange of ILC. Power is no longer simply transferred from one side to the other. The free flow of power within the entire network is realized, which increases the reliability of the system in islanding mode. The simulation results show that under the proposed control

strategy, the hybrid microgrid can operate stably in DC sub-network islanding mode, AC sub-network islanding mode, AC-DC mixed islanding mode and grid-connected mode. Better load sharing can be realized in the whole network.

3) A smooth transition method based on islanding signal is proposed. By detecting islanding signal, the state of regulator is updated to ensure no step change of regulator state at transition instant. Through the comparison of direct transition method, traditional smooth transition method and the novel smooth transition method based on islanding signal proposed in this thesis, it is shown that the smooth transition method based on islanding signal can ensure no step change of regulator state at any transition instant. The transition impact is smaller than that of direct transition method and traditional transition method. The transition time is shorter, as well. Finally, based on the proposed method, the influence of load on smooth transition is also studied. Simulation result shows that the impact increases with the increase of unbalance power in sub-networks at transition instant.

5.2 Future plan

In this thesis, based on the proposed hybrid microgrid structure in a small factory, the researches on control strategy and smooth transition are carried out. In this model, most of the loads are resistive or constant power loads. The loads such as inductive and capacitive loads have not been taken into consideration. It cannot fully show the load condition in real life. The following research should be conducted on load modelling. The application of secondary regulator of voltage droop need to be discussed as well. Topics like hybrid microgrid structure, access of more DGs, load distribution, etc still require further study.

6 REFERENCES

[1] R. H. Lasseter. CERTS Microgrid Laboratory Test Bed[J]. IEEE Transactions on Power Delivery, 2011, 26(1): 325-332.

[2] R. H. Lasseter, P. Paigi. Microgrid: a conceptual solution. 2004 IEEE 35th Annual Power Electronics Specialists Conference (IEEE Cat. No.04CH37551), 2004, 6: 4285-4290.

[3] Lu Z, Wang C, Min Y． Microgrid Research Review [J]. Automation of Electric Power Systems, 2007(19)：100-107．

[4] H. Nikkhajoei, R. H. Lasseter. Distributed Generation Interface to the CERTS Microgrid[J]. IEEE Transactions on Power Delivery, 2009, 24(3): 1598-1608.

[5] S. Bae, J. O. Kim. Reliability Evaluation of Customers in a Microgrid[J]. IEEE Transactions on Power Systems, 2008, 23(3):1416-1422.

[6] Li F, Li R, Zhou F． Micro-grid technology and engineering applications [M]. China Electric Power Press, 2013．

[7] Wang C． Microgrid Analysis and Simulation Theory [M]. Science Press, 2013.

[8] Chen Z, Wang K, Li Z, et al. A review on control strategies of AC/DC micro grid[C]// IEEE International Conference on Environment and Electrical Engineering and 2017 IEEE Industrial and Commercial Power Systems Europe. IEEE, 2017:1-6.

[9] Zhang K. Research on Operation Control Strategy of AC/DC Hybrid Microgrid[D]. North China Electric Power University, 2016.

[10] Nasirian V, Davoudi A, Lewis F L, et al. Distributed Adaptive Droop Control for DC Distribution Systems[J]. IEEE Transactions on Energy Conversion, 2014, 29(4):944-956.

[11] Zhang H, Wang Y, Wang Lin. DC Microgrid Coordinated Control Based on DC Bus Voltage Signals [J]. China Power, 2015, 48(11):110-116.

[12] Gao P, Sun A, Liu J. Research on Smooth Switching Control Strategy of Optical Storage Microgrid[J]. Scientific Innovation, 2016(31):32-33.

[13] Li X，Guo L，Wang C．An Overview of Key Technologies for DC Microgrid [J]. China Journal of Electrical Engineering, 2016(01):2-17.

[14] Lou B，Zhou Z．An Overview of Micro-power Supply Control in AC Microgrid [J]. China Power, 2016(S1):138-143.

[15] J. A. Pecas Lopes, C. L. Moreira, A. G. Madureira. Defining control strategies for analysing microgrids islanded operation. 2005 IEEE Russia Power Tech, 2005: 1-7.

[16] Lou B，Zhou Z．An Overview of Micro-power Supply Control in AC Microgrid [J]. China Power, 2016(S1):138-143.

[17] J. M. Guerrero, J. C. Vasquez, J. Matas, et al. Hierarchical Control of Droop-Controlled AC and DC Microgrids—A General Approach Toward Standardization[J]. IEEE Transactions on Industrial Electronics, 2011, 58(1): 158-172.

[18] Ai X, Deng Y, Li J. Master-slave control strategy for microgrid distributed power supply[J]. Journal of North China Electric Power University (Natural Science), 2015, 42(1):1-6.

[19] Han P，Zhang H，Du Q．Microgrid master / slave control strategy analysis and research [J]. Low-voltage electrical appliances, 2012 (14): 22-26.

[20] Zhang X, Zhang X, Kong B. Research on Multi-master-slave Control Strategy of Microgrid[C]//2013 National Conference on Protection and Control. 2013:20-25.

[21] Du Z, Ou Y, Zhou C. Master-slave Control Strategy for Novel Island Microgrid[J]. Journal of Electrical Engineering, 2015, 10(4):53-61.

[22] M. C. Chandorkar, D. M. Divan, R. Adapa. Control of parallel connected inverters in standalone AC supply systems[J]. IEEE Transactions on Industry Applications, 1993, 29(1): 136-143.

[23] Su H, Cao W, Sun J. Micro-grid coordination control strategy based on improved droop control[J]. Power System Protection and Control, 2014(11):92-98.

[24] Jing L, Huang X, Wu X. Research on Improved Microsource Droop Control Strategy[J]. Journal of Electrical Engineering Technology, 2014, 29(2):145-152.

[25] Zheng Y，Chen M，Li C．Self-adaptive adjustment of droop coefficient microgrid control strategy [J]. Power System Automation, 2013(07): 6-11.

[26] Zhou X, Rong F, Lu Z. Virtual Power V/f Droop Control Strategy Using Coordinate Rotation in Low-voltage Microgrid[J]. Electric Power System Automation, 2012, 36(2):47-51.

[27] Wu Z, Song W, Wei Y. Low-voltage microgrid virtual coordinate transformation droop control strategy [J]. Power System Protection and Control, 2014(8):101-107.

[28] Zhang P，Han X，Zheng R．Research on Operation Strategy of AC/DC Hybrid Microgrid Based on Energy Storage Control [J]. East China Electric Power, 2013(05): 967-972.

[29] Wu B，Xie W，Ye H．AC and DC hybrid microgrid DC bus voltage stability control technology [J]. China Power, 2017 (01): 62-66.

[30] R. Majumder. A Hybrid Microgrid With DC Connection at Back to Back Converters[J]. IEEE Transactions on Smart Grid, 2014, 5(1): 251-259.

[31] P. Karlsson, J. Svensson. DC bus voltage control for a distributed power system[J]. IEEE Transactions on Power Electronics, 2003, 18(6): 1405-1412.

[32] Hui M．AC and DC hybrid microgrid collaborative control and active load response strategy [D]. Harbin, Harbin Institute of Technology, 2015.

[33] Yang Y，Zhou K．Photovoltaic cell modeling and MPPT control strategy [J]. Chinese Journal of Electrical Engineering, 2011(S1):229-234.

[34] Wang Z．Power Electronics Technology [M]. Machinery Industry Press. 2009.

[35] Ren X．Proton exchange membrane fuel cell research progress [J]. Chinese Engineering Science, 2005(01):86-94.

[36] Zhang L，Pan M，Quan S．An Overview of Proton Exchange Membrane Fuel Cell System Modeling and Control [J]. Journal of Wuhan University of Technology (Information & Management Engineering), 2007(04):1-6.

[37] Yi B．Fuel Cell - Principles, Technology, Applications [M]. Chemical Industry Press, 2003.

[38] K. Strunz, H. Louie. Cache energy control for storage: Power system integration and education based on analogies derived from computer engineering[J]. IEEE Transactions on Power Systems, 2009, 24(1): 12-20.

[39] Liao J，Li J．Lead-acid battery charging technology review [J]. Battery, 2010(03): 132-135+139.

[40] Zhang L，Sun K，Wu T．Based on photovoltaic power generation DC microgrid energy transformation and management [J]. Chinese Journal of Electrotechnics, 2013(02):248-254.

[41] Guo J，Tang X，Qi Z．Super capacitor and battery hybrid energy storage system in the application of micro-grid [J]. Power System Automation, 2010(12):85-89.

[42] Zhang X，Zhang C．PWM Rectifier and Its Control [M]. Machinery Industry Press, 2012.

[43] Y. Xia, Y. Peng, P. Yang, et al. Distributed Coordination Control for Multiple Bidirectional Power Converters in a Hybrid AC/DC Microgrid[J]. IEEE Transactions on Power Electronics, 2017, 32(6): 4949-4959.

[44] Zhu Y, Jia L, Cai B. Overview of Topology and Basic Control Strategies for AC/DC Hybrid Microgrid[J]. High Voltage Technology, 2016, 42(9):2756-2767.

[45] Jia L, Zhu Y, Du S. AC/DC Microgrid Interconnect Converter Control Strategy[J]. Electric Power System Automation, 2016, 40(24):98-104.

[46] Bi D, Zhou W, Dai Y. Seamless Switching Strategy for Energy Storage Converters in AC/DC Hybrid Microgrid[J]. Automation of Electric Power Systems, 2016, 40(10):84-89.

[47] Wu Z, Song W, Zhang J. Low-voltage microgrid smooth switching virtual coordinate transformation droop control strategy [J]. Electrical Applications, 2014(5):60-64.

[48] Xu J, Lu W, Wu L. Low-voltage Microgrid Inverter and Off-grid Smooth Switching Control[J]. Science Technology and Engineering, 2017, 17(9):36-43.

[49] Nasirian V, Davoudi A, Lewis F L, et al. Distributed Adaptive Droop Control for DC Distribution Systems[J]. IEEE Transactions on Energy Conversion, 2014, 29(4):944-956.

[50] Sun R, Song Y, Li J. Voltage droop control method of DC microgrid[J]. Heilongjiang Electric Power, 2014, 36(2):122-125.

[51] Xie W, Zhu Y, Du S. Power Control of Interconnected Converters in AC/DC Hybrid Microgrid[J]. Electric Power Construction, 2016, 37(10):9-15.

[52] Zhang T, Li X. Smart Grid Islanding/Networking Smooth Switching Control Strategy with Photovoltaic Sources[J]. Power System Technology, 2015, 39(4):904-910.

[53] Fu Y, Huang L, Zhao J. Micro-grid Smooth Switching Control Method Based on Controller State Following[J]. Journal of Shanghai University of Electric Power, 2014, 30(6):495-499.

[54] Li Y, Li Y, Cheng Z. Research on Smooth Switching Control Strategy of Microgrid Based on Master-Slave Control[J]. Electric Measurement & Instrumentation, 2016, 53(24):44-49.

[55] Zheng T, Chen L, Mei S. Master-slave Microgrid Smooth Switching Control Considering Timing Coordination[J]. Electric Power & Energy Management Technology, 2014(10):44-49.